Postprint of: Śmiechowski M. , Gojło E. , Stangret J., Systematic Study of Hydration Patterns of Phosphoric (V) Acid and Its Mono-, Di-, and Tripotassium Salts in Aqueous Solution, JOURNAL OF PHYSICAL CHEMISTRY B, Vol. 113, Iss. 21 (2009), pp. 7650–7661

Systematic Study of Hydration Patterns of Phosphoric(V) Acid and Its Mono-, Di-, and Tripotassium Salts in Aqueous Solution

Maciej Śmiechowski, Emilia Gojło, and Janusz Stangret*

Department of Physical Chemistry, Chemical Faculty, Gdańsk University of Technology,

Narutowicza 11/12, 80-233 Gdańsk, Poland

E-mail address: msmiech@chem.pg.gda.pl.

RECEIVED DATE:

* To whom correspondence should be addressed. Phone: (+48) 58 347 1283. Fax: (+48) 58 347 2694.

E-mail address: msmiech@chem.pg.gda.pl.

Fourier transform infrared (FTIR) spectroscopy of the OD band of HDO molecules has been applied to perform a systematic study of various phosphate forms in the order of decreasing protonation: H_3PO_4, KH_2PO_4, K_2HPO_4, K_3PO_4. HDO isotopically diluted in H_2O has been prepared by adding adequate amounts of D_2O to aqueous solutions in ordinary water. The difference spectra procedure has been applied to remove the contribution of bulk water and thus to separate the spectra of solute-affected HDO. The position at maximum of the principal anion-affected HDO band for potassium phosphates moves in the order KH_2PO_4 (2478 cm^{-1}) > K_2HPO_4 (2363 cm^{-1}) > K_3PO_4 (2301 cm^{-1}), i.e. decreases with increasing solute basicity and charge. The number of moles of water affected by one mole of solute (N) equals 11.0, 13.8 and 16.2, respectively. Phosphoric acid affects statistically 13.9 water molecules and appears to be a "structure making" solute in water. The isotopic substitution with deuterium occurs also on the phosphate anions and phosphoric acid. The thus formed P-O-D groups interact with water molecules via strong hydrogen bonds and the relative strength of this interaction increases with increasing solute acidity. The plausible assignments of OD bands of HDO have been confirmed by calculating equilibrium structures of small aqueous clusters of the studied individua utilizing Density Functional Theory (DFT). Further interpretation of the energetic and structural properties of hydrating water is enabled by calculating intermolecular interaction energy of water and probability distributions for interatomic oxygen-oxygen distance.

Keywords: FTIR spectroscopy, solute-affected spectra, DFT calculations, phosphoric(V) acid, potassium phosphates(V)

Introduction

The phosphate anions and their organic derivatives are of crucial importance in biological systems.[1] Their universal role in the proper functioning of living organisms cannot be underestimated. Phosphates also find numerous applications in the agricultural industry (as fertilizers), food industry (as soft drink additives) and cosmetic industry (as components in detergents and cleaning agents). Particularly, the $H_2PO_4^-$ and HPO_4^{2-} anions play a key role in the metabolic pathways, since at physiological pH these are the most abundant forms present in an aqueous solution.[2] The phosphate buffer system, comprised of both these anions, is one of the major pH controlling systems in the human body, particularly important in the intracellular fluid and urine.[3] Nevertheless, all other phosphate forms present at varying acidity of the medium should also be taken into account and thoroughly studied.

Ionic equilibria between the phosphate anions are complicated and involve multiple species and complexes.[2] Phosphoric(V) acid, like most polyprotic inorganic oxoacids, is characterized by dissociation constants rising by about 5 pK_a units in each consecutive dissociation step (2.16, 7.21 and 12.32).[4] One of the practical consequences is that for aqueous H_3PO_4 the contribution of further dissociation reactions beyond the first one is so small that it might as well be disregarded for all practical purposes, making H_3PO_4 essentially a "monoprotic" acid. However, in the case of PO_4^{3-}, as well as H_3PO_4, the contribution of $H_2PO_4^-$ or HPO_4^{2-}, respectively, is non-negligible, due to extensive dissociation or hydrolysis of the solute. The pH dependence of phosphate speciation is important especially in conditions near to physiological and knowledge of the relative proportions of the phosphate anions has direct biochemical relevance, for example at pH around 7, where $H_2PO_4^-$ and HPO_4^{2-} are present in approximately equivalent amounts.[2]

Strong monoprotic acids are known to show broad, pronounced, but poorly defined features in the vibrational spectra, known as the "continuum of absorbance."[11,12] On the contrary, vibrational spectra of aqueous phosphoric acid at moderate concentrations are almost devoid of these features.[2] More pronounced continuum, however, was found at the 1:1 H_3PO_4 to H_2O ratio.[12] A strongly hydrogen-bonded network was found in aqueous H_3PO_4 in diffraction experiments,[13] although the reported hydration number of 4 seems rather small at first sight.[14]

It is well-known that the strength of anionic hydration (measured by the mean water-water interaction energy in the hydration sphere) depends linearly on the polarizing power of the anion (i.e., its charge to ionic radius ratio) for most oxoanions.[5] Therefore, the water structure-making properties of phosphate

anions should increase with increasing charge. This behavior was confirmed both experimentally[6] and computationally.[7] The PO_4^{3-} anion is usually described as "strongly hydrated in aqueous solutions."[8,9] Nevertheless, the tendency for large hydration numbers in the first hydration shell was shared by all anionic phosphate forms in previous investigations, regardless of the degree of protonation,[6,9,10] and in some cases a partially ordered second hydration shell could be deduced from the data.[10]

Fourier transform infrared (FTIR) spectroscopy is a useful technique allowing the study of solute hydration. By using isotopic dilution technique, HDO spectra can be obtained that are free from interpretative and experimental difficulties connected with H_2O spectra.[15-17] This technique has been successfully applied to study a wide range of electrolytes.[5] The application of the difference spectra method for results' analysis allows separation of the spectra of solute-affected HDO from the bulk solvent.[18-21] Here we apply FTIR spectroscopy of the OD band of HDO molecules to perform a systematic study of various phosphate forms in the order of decreasing protonation: $H_3PO_4 \rightarrow KH_2PO_4 \rightarrow K_2HPO_4 \rightarrow K_3PO_4$. Potassium is the most suitable cation of choice in this study, since its tendency to form ion pairs with phosphate anions appears to be negligible.[22] Furthermore, the way it affects HDO was characterized previously in detail.[23] Systematic investigations of the phosphate(V) system are uncommon in the recent literature[2] and the isotopic dilution technique is applied here for the first time for this purpose. Additionally, we calculated equilibrium structures of small aqueous clusters of the studied individua utilizing Density Functional Theory (DFT) with a hybrid exchange-correlation functional to confirm the plausible assignments of OD component bands in the affected HDO spectra.

Experimental Section

Phosphoric(V) acid (H_3PO_4 85% aq., pure p.a., POCh S.A., Poland) and its potassium salts – dihydrogenphosphate (KH_2PO_4, pure p.a., POCh S.A., Poland), hydrogenphosphate (K_2HPO_4, pure p.a., POCh S.A., Poland) and phosphate (K_3PO_4, 97%, Aldrich) were used as supplied. D_2O used in the preparation of solutions was provided by Institute of Nuclear Investigation, Poland (99.84% isotopic purity).

Stock solutions were prepared by dissolving weighted amounts of respective solutes in double-distilled water. The series of solutions were prepared by dissolving weighted amounts of respective stock solution in double-distilled water. Sample solutions were made by adding 4% (by weight) of D_2O relative to H_2O and reference solutions by adding the same molar amounts of H_2O. Densities of the salt

solutions were measured with an Anton Paar DMA 5000 density meter at 25.000±0.001 °C. Densities of the H_3PO_4 solutions were interpolated from available literature data.[24] The solution series included samples of the following molalities: H_3PO_4 – 0.0389, 0.0583, 0.0976, 0.1938, 0.3864, 0.7745, 0.9599 mol·kg^{-1}; KH_2PO_4 – 0.0959, 0.1915, 0.2877, 0.5820, 0.7714, 0.9993 mol·kg^{-1}; K_2HPO_4 – 0.0962, 0.1923, 0.2888, 0.3841, 0.5836, 0.7700, 0.9599 mol·kg^{-1}; K_3PO_4 – 0.1917, 0.3808, 0.5789, 0.7680, 0.9659 mol·kg^{-1}.

FTIR spectra were recorded on an IFS 66 Bruker spectrometer. 256 scans were made with 4 cm^{-1} resolution. A cell with CaF_2 windows was employed. The path length was 0.0299 mm, as determined interferometrically. The temperature, monitored by a thermocouple inside the cell, was kept at 25.0±0.1 °C by circulating thermostated water through mounting plates of the cell. The spectrometer was purged with dry air free of carbon dioxide.

Spectral Data Analysis

The spectra have been handled and analyzed by commercial programs GRAMS/32 4.01 (Galactic Industries Corporation, Salem, USA) and RAZOR (Spectrum Square Associates, Inc., Ithaca, USA) run under GRAMS/32.

Spectral data have been analyzed following the published procedures, leading to separation of the spectrum of solute-affected water only, basing on the spectra of the entire solution series and the bulk HDO spectrum.[20,21] The algorithm is based on the assumption that water in solution may be divided into additive contributions of bulk (*b*) and solute-affected (*a*) water. The vibrational spectrum of the latter, ε_a, may be calculated for each wavenumber from Eq. (1), using the pure HDO spectrum, ε_b, the "affected number", *N*, and the derivative of absorption vs. molality in the infinite dilution limit. *M* denotes the mean molar mass of water (H_2O + 4% D_2O).

$$\varepsilon_a = \frac{1}{NM}\left(\frac{\partial \varepsilon}{\partial m}\right)_{m=0} + \varepsilon_b \qquad (1)$$

An approximation of the experimental spectra $\varepsilon(\nu_i)$ vs. molality *m* at each wave-number ν_i by the least squares method allows the calculation of the respective derivative. Normally, low-order polynomial provides a satisfactory fit for this purpose.[21]

Eq. (1) contains two unknowns: ε_a and *N*. The latter parameter is equal to the number of moles of water affected by one mole of solute. It should not be confused with "hydration number" (in the sense

of the parameter obtained from diffraction experiments or molecular dynamics simulations). *N* is close to hydration number derived from "direct" methods only when the solute-affected HDO band differs sufficiently from the bulk HDO band, either in position or in half-width. Otherwise, affected number is usually lower than the hydration number. However, the solute-affected HDO spectrum carries structural and energetic information about greater number of solvent molecules surrounding the solute molecule, depicting the water status in a somewhat "condensed" form.[21] This, along with the short time scale of vibrational spectroscopy (ca. $7.5 \cdot 10^{13}$ Hz in the range of OD stretching vibration), is the main cause of high sensitivity of the method to differentiate various states of solvent molecules in the solution.

The proper value of affected number is found basing on the published algorithm.[20,21] In brief, the trial solute-affected water spectrum for a given *N* value is fitted using the baseline, analytical bands and the bulk water spectrum. The minimal number of analytical bands, which give an adequate fit, is considered as the right number of component bands. This can be verified by examination of the second derivative of the trial affected spectrum: the plot of this derivative shows minima that approximately illustrate the positions and the number of underlying component bands. The product of Gaussian and Lorentzian peak functions is used as the starting analytical band shape, but it might be replaced later by a pure function for a given band if the contribution of the other component is found negligible. All parameters (including Gaussian to Lorentzian ratio) are unconstrained during the fit, with the exception of bulk HDO spectrum, for which only intensity is allowed to vary. The maximum value of *N*, for which the solute-affected water spectrum still contains a negligible amount of the bulk water spectrum (the practical threshold value is set at 0.5% of the total integrated intensity of the ε_a spectrum) is considered as the "true" value of *N*, and the corresponding ε_a spectrum as the "true" affected water spectrum. Thus, both unknowns are obtained simultaneously.

Computational Details

Medium-sized aqueous clusters, $X(H_2O)_n$, n = 7-9, X = H_3PO_4, $H_2PO_4^-$, HPO_4^{2-} or PO_4^{3-}, were used as model systems in the calculations. The clusters studied here are larger than those found in most of previous investigations.[7,10,25-28] Initial structures of all studied systems showed C_1 symmetry and no symmetry constraints were imposed during geometry optimizations. *Ab initio* calculations were performed with the use of standard basis set 6-311++G(d,p).[29-31] Employed basis set is of the triple-*zeta* type and is augmented with polarization and diffuse functions on all atoms. Density Functional Theory

calculations utilized the hybrid B3LYP combination functional.[32,33] Numerical integrations were done with an *UltraFine* (99,590) grid. The Berny algorithm[34] with *Tight* convergence criteria was used for optimizations. Vibrational analysis was performed on optimized clusters to check for absence of imaginary frequencies and thus confirm the existence of local energetic minima.

Gas-phase cluster structures were subsequently used as starting points for geometry optimization in the self-consistent reaction field (SCRF) approach. The polarizable continuum solvation model (PCM) was used,[35-37] with United Atom Topological Model applied on atomic radii of the UFF force field (UA0). The GDIIS method[38] was used in the PCM calculations to speed up the optimization process.

All calculations were performed with the Gaussian 03 system.[39] GaussView 3.0 (Gaussian, Inc., Wallingford, CT) served as an interface for visualization.

Results

Composition of the Studied Solutions. The experimental pK_a values of phosphoric(V) acid are 2.16, 7.21 and 12.32, as already mentioned.[4] The knowledge of these dissociation constants alone is sufficient to predict the concentration of any given form at a specific pH value.[2] This problem may be also approached from another point of view: what is the distribution of species if a single solute is dissolved in water at a given nominal concentration? Both of these questions may be answered simultaneously using the same set of equations, although the second one is more important for the spectral data analysis presented in this work. The fundamental relations necessary for resolution of these problems are derived in the supporting information to this paper.

Figure 1 presents the relative concentration profiles of the studied phosphate forms at varying pH. The regions where pH of the studied solutions is expected are additionally highlighted. The pH of the most concentrated stock solutions was checked with a Schott Handylab pH 11 pH-meter equipped with a N6000A glass microelectrode at ambient temperature and found to differ no more than 0.2 units from the predicted values. It is immediately seen that for $H_2PO_4^-$ and HPO_4^{2-} these fall into the regions of maximal abundance of the respective anion, which is estimated to exceed 99.4% of the total phosphate concentration. The situation is different for the two other phosphate forms, however, as the contribution of dissociation (in the case of H_3PO_4) and hydrolysis (in the case of PO_4^{3-}) is non-negligible and may reach ca. 30% for the solution concentrations considered here. Sometimes it is convenient to disregard the phosphate speciation, as was for example done in neutron diffraction data analysis, where K_3PO_4

was assumed to yield PO_4^{3-} only.[6] However, the possible significance of the presence of different phosphate forms for our analysis of vibrational spectra is further evaluated in the "Discussion" section.

Solute-Affected HDO Spectra. The measured HDO spectra in the OD stretching vibration region for aqueous solutions of the four studied phosphate solutes are shown in Figure 2 with the $(\partial\varepsilon/\partial m)_{m=0}$ derivatives superimposed. The linear dependence of ε on m at each wavenumber was found adequate with the exception of K_3PO_4, for which quadratic function was necessary for better description. The derivatives are also presented together in Figure 3(a) for better comparison of the solutes. The solute-affected HDO spectra determined on the basis of these derivatives are shown in Figure 3(b) and compared with the bulk HDO spectrum. The affected numbers (N) were found equal to 13.9 for H_3PO_4, 11.0 for KH_2PO_4, 13.8 for K_2HPO_4 and 16.2 for K_3PO_4. These results are larger than for most electrolytes in an aqueous solution,[5] but undoubtedly the phosphate anions exhibit large coordination numbers in water.[6,10] On the other hand, summing up the coordination numbers obtained by diffraction methods for K^+ and the studied anions,[6,40,41] we could expect total hydration numbers much higher than the above N values. However, the correspondence between affected number and hydration number is perfect only under certain circumstances and usually N is lower than the experimentally obtained hydration number, so that the affected spectra describe the water status in a "concentrated" form.[21]

The affected HDO spectra from Figure 3(b) are shown in Figure 4 after decomposition into analytical bands. Selected parameters of these bands are collected in Table 1. At first sight, the phosphate anions appear to be potent "structure makers" in an aqueous solution, a situation uncommon for anions, with only a few exceptions.[5,42] The most intense component bands were significantly red-shifted from the bulk HDO position (2509 cm^{-1}), which could not be attributed to the cation influence, since alkali metals are known to slightly blue-shift the HDO spectrum.[5,23] The H_3PO_4-affected HDO spectrum resembles closely that of the dihydrogenphosphate salt, without noticeable anomalies. Specifically, no "continuum"-like features[11,12] or extremely red-shifted component bands[43] could be detected.

A more detailed analysis of affected HDO spectra is found in the "Discussion" section below.

Cluster Geometries in the Gas Phase and in an Aqueous Solution. The structures of the studied clusters after geometry optimization in the gas phase are shown in Figure 5. The optimized structures in Cartesian coordinates, as well as electronic energies and zero point energies of the clusters are available as Supporting Information to this paper. Since the parameter most useful in the comparison with the experimental affected HDO spectra is the hydrogen bond (H-bond) length, measured by interatomic

oxygen-oxygen distance (R_{OO}), only this is shown in Table 2, averaged over hydrogen bonds in different molecular situations in all clusters of a given solute.

The molecular situations for hydrogen bonding discriminated in Table 2 include: (a) H-bonds donated to water by a hydrogen atom covalently bonded to one of the phosphate oxygens (denoted P-OH···OH_2); (b) H-bonds donated from a water molecule to one of the "free" (i.e., without covalently bonded hydrogen) oxygen atoms of the phosphate (P=O···H-OH); (c) H-bonds between the hydrating water molecules (HO-H···OH_2); (d) H-bonds donated from a water molecule to one of the "acidic" (i.e., with covalently bonded hydrogen) phosphate oxygens (P-O(H)···H-OH); and (e) the "bridging" water molecules in the case of PO_4^{3-}, H-bonded to two "free" phosphate oxygens simultaneously (P=O···H-OH···O=P).

The PCM-optimized clusters mostly kept the gas-phase geometry, although with two notable exceptions. For the hydrogen phosphate, the H-bond donated by the P-O-H group of the anion was absent in the clusters with 7 and 8 H_2O molecules, while for PO_4^{3-} the "bridging" waters were also absent in all clusters, moving away to form a more "regular" cage. The H-bond lengths generally shortened in the dielectric medium, as shown in Table 2, but with a few exceptions, most importantly the P=O···H-OH bonds for all the solutes. It is also noticeable that the groups of H-bonds are better defined in PCM, as evidenced by significantly lower values of standard deviations for average R_{OO}.

The R_{OO} value can be easily transformed to the OD band position of HDO (ν^{o}_{OD}) with the aid of empirical relations. Eq. (2) linking ν^{o}_{OD} to R_{OO} was established on the basis of vibrational spectra and neutron diffraction measurements on crystalline hydrates.[44]

$$\nu^{o}_{OD} / cm^{-1} = 2727 - \exp[16.01 - 3.73(R_{OO} / Å)] \qquad (2)$$

The calculated frequencies (ν^{c}_{OD}) for the studied solutes are shown in Table 2. Previously, we found that such empirical frequencies correlate adequately with experimental HDO spectra and facilitate their easier interpretation.[42,43]

Discussion

The H-bond arrangements and lengths in the different phosphate clusters found by us are generally in agreement with available experimental and computational data. However, reports of investigations on moderately concentrated aqueous solutions of H_3PO_4 are scarce in the literature. Two available X-ray studies predict R_{OO} for acid-water H-bonded interaction equal to 2.72-2.73 Å.[13,14] Also, a hydration

number of 4 for H_3PO_4 derived by diffraction[14] seems rather low, when compared with the clusters from Fig. 5. However, by considering together the two equally represented P-OH···OH_2 and P=O···H-OH situations (Table 2), we obtain an average $R_{OO,PCM}$ equal to 2.72 Å, in excellent agreement with the experimental results. Therefore, we suspect that the diffraction picture naturally averages two different molecular situations, resulting in a mixed final value.

On the other hand, computational and structural studies of other aqueous phosphates are more available. Several ab initio and molecular dynamics (MD) investigations were performed previously for $H_2PO_4^-$,[7,10,26,28,45] HPO_4^{2-},[7,10,27,45] and PO_4^{3-} anions.[7-10,25] Moreover, recent neutron scattering measurements for all three anions provide a detailed characteristic of their hydration spheres.[6] Some previous diffraction results were also reviewed.[40,41] Phosphates were mainly studied computationally with a limited number of water molecules forming a cluster,[7,10,25-28] making these results of lesser value for comparison with the present work. However, a single static calculation for PO_4^{3-} with up to 18 hydrating waters is available.[8] Also MD studies provide reliable data for large number of water molecules surrounding the solute.[9,10,45]

In most of the smaller clusters studied previously, the hydrating water molecules often preferred the "double donor" configuration, meaning that H_2O was H-bonded to the anion with both its hydrogen atoms.[7,10,25-28] By contrast, such an arrangement is relatively rare in our optimized clusters (Fig. 5), in which water molecules rather build up a larger H-bonded cage around the solute, isolated "double donor" H_2O in the case of PO_4^{3-} in the gas phase being the only exception. In small $H_2PO_4^-$ clusters, the $R_{OO,gas}$ values at the MP2/6-31+G* level were spread rather randomly around ca. 2.9-3.0 Å, with some outlying values at 2.7 Å, attributed to donor H-bond of the "donor acceptor" H_2O molecules.[26] The significance of this arrangement was confirmed later with an abundant basis set.[28] In our large clusters, devoid of such H_2O molecules, H-bonds donated by water to $H_2PO_4^-$ are actually longer on average from those accepted by water from the anion by at least 0.1 Å (in PCM). In another study, using the same level of theory as the present one, $R_{OO,gas}$ as high as 2.96 Å was found for single hydrating "double donor" water.[7] For HPO_4^{2-}, Pye and Michels found that $R_{OO,gas}$ values were spread between 2.8 and 2.9 Å in n = 1-6 clusters, being shorter than for $H_2PO_4^-$.[27] As before, some even shorter H-bonds close to 2.7 Å were found. "Double donor" H_2O arrangement was again mostly preferred.[27] At the level of theory applied by us, for a single water molecule in this position $R_{OO,gas}$ was equal to 2.78 Å, not far from our average for the P=O···H-OH group.[7] In the MD study of both just mentioned anions, they were

concluded to resemble PO_4^{3-} to a large extent, at least from OO radial distribution functions point of view.[10]

For the latter anion, a comparatively larger amount of data is available. Both classical MD and ab initio MD simulations predicted phosphate oxygen to water oxygen distance to be ca. 2.75 Å, with the coordination number of the anion ranging from 12 to 16.[9,10] Static ab initio calculations also resulted in a complete first hydration sphere consisting of 12 H_2O molecules.[8] The hydration number derived from neutron diffraction was in turn 15 ± 3, but the phosphate-water R_{OO} was not separated in the analysis from the bulk water R_{OO}.[6] Again, in smaller aqueous clusters, the "double donor" water arrangement was commonly found, with R_{OO} equal 2.67-2.8 Å.[7,10,25] We might therefore conclude that for our PO_4^{3-} clusters presented here, ion-water R_{OO} is slightly lower than previously found, and the building up of the first hydration shell is incomplete, however, as shown later, this does not limit the applicability of cluster structures for HDO spectra analysis.

The above considerations about the optimal cluster structures are meant to facilitate the interpretation of component bands in the affected HDO spectra from Fig. 4. Most of the previous vibrational spectroscopic investigations of phosphate aqueous solutions concerned primarily either the anion intramolecular modes,[7,8,22,25,45-49] or the "continuum of absorbance" between stretching and bending modes of water.[11,12] However, some of these works mention also the intramolecular P-O-H phosphate modes in solution[7,46-48] or the perturbation of water stretching fundamental by the phosphate.[8] An excellent work of its own is the extensive report by Baril, Max and Chapados, devoted to vibrational spectra of phosphate aqueous solutions depending on their pH in the entire mid-infrared region.[2]

Each of the four phosphates exhibits four analytical components in its affected spectrum (Fig. 4), with their positions remaining very similar for all the solutes. Also, the analysis of the optimal cluster structures focuses on four distinct groups of H-bonds in the ion surroundings (Table 2). The straightforward correspondence between theory and experiment seems attractive; however, some precautions must be taken to not oversimplify the model arising from spectral data and calculations.

To verify the optimal number of the component bands in the affected spectra, the second derivatives of these spectra were calculated. The Bayesian derivative algorithm implemented in RAZOR for GRAMS/32 was used for this purpose. The minima on such plots show the approximate location of underlying component bands in a composite spectrum; see Fig. 3 (c). The second derivatives shown in this figure contain some spurious peaks above 2700 cm^{-1} and below 2100 cm^{-1}, resulting from features

other than the OD band itself. In the OD stretching region they do contain, however, several clearly visible minima. The picture is totally unambiguous for K_3PO_4, where four clearly marked minima can be seen. Also for KH_2PO_4 four minima are discernible, although the most red-shifted one is quite shallow. In the case of K_2HPO_4 three minima are apparent, but the fourth feature manifests itself only as an inflection in the curve at ca. 2330 cm^{-1}. The picture is, however, less clear for H_3PO_4, where the first two minima are apparent, but the other two are hard to locate. A very shallow minimum appears above 2200 cm^{-1}, but the remaining feature is again only an inflection at ca. 2350 cm^{-1}, this time very slight. Therefore, the presence of four analytical peaks is confirmed for all the studied solutes, apart from phosphoric acid. Although the application of four analytical peaks seems questionable for H_3PO_4, the overall shape of the affected spectrum, very similar to the KH_2PO_4 case, as well as the presence of some minor features in the regions, where other solutes display proper minima, encouraged us to apply the same number of analytical peaks as for the other solutes.

In search of the correct band assignment we focus first on the P-OH···OH_2 group of H-bonds. It seems reasonable to suspect that the stretching mode of the proton in this H-bond should directly depend on the acidity of the solute. To verify this hypothesis, a plot of the OD band position vs. pK_a of the solute as in Figure 6(a) is helpful. It is immediately visible that the average calculated wave number (ν^c_{OD}) is linearly correlated with pK_a, nearly perfectly (R^2 = 0.9997) for the gas phase calculations and slightly less so (R^2 = 0.9832) for the PCM ones. Additionally, the experimental bands at 2440 cm^{-1} for K_2HPO_4 and 2347 cm^{-1} for KH_2PO_4 are practically coincident with the PCM band positions. The ν^o_{OD} values given previously for deuterated anions in D_2O were some 100 cm^{-1} lower (2300 cm^{-1} for K_2DPO_4 and 2200 cm^{-1} for KD_2PO_4), but for rather concentrated solutions.[47,48] The assignments for ν_{OH} of phosphates based on ATR spectra would give a rough estimate of ca. 2050 cm^{-1} for ν^o_{OD} of all acidic phosphates[2] (basing on an OH vs. OD stretch correlation for solid hydrates.)[50] Our experimental spectra are, however, devoid of any visible spectral features in this region. Considering the close similarity of PCM calculations and respective experimental bands, we might unequivocally assign them to the H-bond in the P-OH···OH_2 group. The situation is less clear for H_3PO_4, where both gas phase and PCM calculations predict ν^c_{OD} equal to ca. 2200 cm^{-1}, while the most red-shifted analytical component is situated at 2310 cm^{-1}. In a previous investigation, ν^o_{OD} for conc. D_3PO_4 in D_2O was indeed found at ca. 2200 cm^{-1}, with a weaker side-band at as low as 1750 cm^{-1}.[47] The corresponding bands for H_3PO_4 in H_2O were ascribed to the "absorbance continuum" characteristic of aqueous acids.[12] We have found previously that the

isotopic decoupling introduced in the system by replacing some of the H atoms by D atoms effectively disrupts such "continua" and results in broad, extremely red-shifted OD stretching bands that can still be resolved into analytical components, though.[43] Such decoupling is present in the studied system as well. Furthermore, some dissociation of H_3PO_4 in the 0.2-1.0 mol·dm^{-3} concentration range might be inferred from the known pK_a, possibly shifting the discussed band towards the $H_2PO_4^-$ position. Finally, the location of this band on the side of a stronger one, composed of the 2524 cm^{-1} and 2441 cm^{-1} analytical bands, might disturb the accuracy of the fitting procedure. On the basis of these considerations, we ascribe the 2310 cm^{-1} component for H_3PO_4 to P-OH···OH_2 H-bonds.

By analogy to the previous case, the strength of the P=O···H-OH H-bond should depend in turn on the basicity of the solute, expressed conveniently as pK_b = 14 – pK_a of the conjugated acid. A respective correlation is plotted in Fig. 6(b). Although the linearity is less pronounced this time, a clear trend for both types of calculations is apparent. For all the studied phosphates, gas phase and PCM ν^c_{OD} values were practically the same (Table 2). Again, the experimental band positions are close to the PCM ones, with larger deviation found for HPO_4^{2-} only. Therefore, a plausible assignment of the P=O···H-OH grouping to the respective analytical components might be made for the three anions. Since most of the anions were studied before in their deprotonated forms, with water molecules acting as hydrogen bond donors, rather than acceptors, the discussed band should be considered as the "principal" affected HDO band for the purpose of comparison with other ions.

It was previously established that the anion-affected HDO band position depends linearly on the polarizing power of the anion (q/r, where q is the ionic charge and r is the ionic radius in aqueous solution.)[5] The anions were found to form discrete chemically significant classes in this respect, e.g. for halides or for polyatomic anions.[5] Ionic radii of the phosphates are well known and the commonly accepted values are 2.00 Å for $H_2PO_4^-$ and HPO_4^{2-}, and 2.38 Å for PO_4^{3-}.[51] Figure 7 illustrates precisely the expected correlation and comparison with other available data included in the figure leads to a conclusion that the phosphate anions form their own independent group.[5] Both polyatomic anions and halide anions form basically two parallel running groups in the figure. Extension of the previously found correlation line determined by oxoanions proves that PO_4^{3-} fits adequately in this group. However, the slope of the relationship for the whole phosphate family is less steep than for the other two lines. This suggests that both hydrogen phosphate anions have more pronounced structure-making properties than expected from their polarizing power. The tentative explanation is that this is caused by

the cooperative effect of hydrogen bonds from water to anion and those from anion to water, which effectively strengthens the whole hydration sphere, causing the observed red shift with respect to other oxoanions.

Unfortunately, we are a bit lacking independent experimental confirmation of the structural interpretation of the above discussed P=O···H-OH band. IR spectra of solid hydrates of the phosphate anions demonstrate bands attributable to the asymmetric ν_{OH} of the hydrating "double donor" water at 3462, 3371 and 3216 cm^{-1}, for $H_2PO_4^-$, HPO_4^{2-} and PO_4^{3-}, respectively.[7] This would correspond to ν^o_{OD} equal to 2552, 2492 and 2396 cm^{-1}, some 100 cm^{-1} larger than in our PCM calculations. This apparent H-bond weakening might be explained by the geometric strain in the "double donor" arrangement, not occurring in linear H-bonds (cf. gas phase calculations for PO_4^{3-} in Table 2). Note, however, that the order and relative spacing of the band positions remain in accordance with the present results. Some indirect confirmation is also offered by the ATR spectra, in which the ν_{OH} of water red shifts as the anion charge is increasing.[2] For PO_4^{3-}, occurrence of the "double donor" hydrating water molecules was observed in MD simulations.[9] Although this arrangement was unstable in our PCM calculations, the gas phase ν^c_{OD} is only marginally higher from the experimental band at 2434 cm^{-1}. Therefore, "double donor" HDO and the presence of some HPO_4^{2-} from hydrolysis of PO_4^{3-} in our opinion explain the background of this band. A straightforward extrapolation of the trend observed for anions to the H_3PO_4 case is impossible due to its unknown pK_b. However, considering the close similarity of the ν^c_{OD} in PCM for the P=O···H-OH group (2506 cm^{-1}) and the experimental band position (2524 cm^{-1}), the interpretation may be carried on by way of analogy.

It is instructive to compare the water-water hydrogen bonds in the case of the anions and phosphoric acid. For anions, especially $H_2PO_4^-$ and PO_4^{3-}, ν^c_{OD} in PCM lies notably close to the experimental bulk HDO band position (2509 cm^{-1}). This is in accordance with the general observation that anions rarely possess truly "structure making" properties in an aqueous solutions.[5] It is readily seen, that the "structure making" effect, if any, is due to favorable anion-water interactions, rather than due to extensive strengthening of the water-water H-bonding. This observation remains valid even for such strongly hydrated anion as OH^-.[42] Therefore, no clear experimental counterpart can be indicated for the predicted water-water interaction in the anionic clusters. If the H-bonding pattern really resembles the average bulk water situation, then the procedure of finding the solute-affected HDO spectrum should cancel this influence out, as it would be subtracted to a large extent with ε_b. In contrast to these

conclusions, the discussed group of H-bonds for H_3PO_4 ($\nu^c_{OD,PCM}$ = 2458 cm^{-1}) finds its close experimental counterpart at 2441 cm^{-1}. Therefore, phosphoric(V) acid might be treated as a true "structure making" solute in water, since it directly influences the strength of water-water H-bonds, not only solute-water ones.

For all the three studied anions, another band situated at 2540-2550 cm^{-1} is also found. It is slightly more intense for HPO_4^{2-} than for the other two anions. Ample experimental evidence confirms that this band is due to water-water interactions in the K^+ hydration sphere.[5,23,42] For alkali metal ions, average ν^o_{OD} for cation-affected water amounts[5] 2533 ± 20 cm^{-1} and our results fall within these limits. The elimination of this cation contribution to the affected HDO spectrum, however, can be achieved only following some arbitrary procedure. The cation-anion separation might be sometimes performed with less arbitrary assumptions, provided the spectrum of cation-affected HDO is known in detail and the anionic and cationic bands are separated enough.[42] For potassium, we have the excellent reference spectrum measured before for its hexafluorophosphate salt, which allowed an almost perfect separation of the cation- and anion-affected HDO bands.[23] For the systems studied here, however, to implement such procedure would pose a great difficulty, as the anion-affected HDO spectrum is broad and intertwined with the cation-affected one (cf. affected spectra from Fig. 3(b), which do not have an unambiguous "double peak" structure). As seen from Table 2, H-bonds of the P-O(H)···H-OH type for "acidic" phosphates also appear in this spectral region, possibly explaining slight blue-shift of the band with respect to its average position.[5] For HPO_4^{2-}, the contribution of the water-water H-bonds within the hydration sphere to the discussed band cannot be ruled out, the more so that it is significantly more intense than for the other two anions (Table 1). Consequently, the separation of the ionic contributions eventually has not been attempted here.

The cationic and anionic contributions manifest themselves also in entirely different spectral region. The "cation+anion" band invoked here was previously attributed to the farthest hydration sphere of the cation, influenced simultaneously by the anion.[23] Its position depends approximately linearly on the position of the anion-affected HDO band.[23] To verify the validity of this approach, we plot in Fig. 8 the most blue-shifted analytical band position for the three anions vs. the position of the principal anion-affected HDO band. Linear fit (R^2 = 0.9927) is in fact firmly justified and the interpretation proposed before remains valid. A similar band appears also in the H_3PO_4-affected HDO spectrum, where it must

originate from entirely different molecular situation. On the basis of our calculations, we attribute it to the H-bonds donated by water to the "acidic" oxygen atoms of the acid molecule (Table 2).

The interpretation of the analytical component bands in the phosphate-affected HDO spectra presented above is conveniently collected in Table 3. Several bands can be ascribed to more than a single interaction, however, the separation of these effects is impossible without strong arbitrary assumptions, as discussed above in detail for some of these cases.

The vital question left unanswered until now is the influence of products of dissociation and hydrolysis in the case of H_3PO_4 and PO_4^{3-}, respectively. As mentioned previously, the speciation curves suggest a maximum of ca. 30% contribution of the other phosphate(V) forms in the case of these two solutes. It has been already suggested that especially the 2310 cm^{-1} band for H_3PO_4 and the 2434 cm^{-1} band for PO_4^{3-} might be significantly influenced by the presence of different phosphate forms. To verify this possible influence on the component band parameters, we performed a subtraction of the affected HDO spectra. Assuming the worst possible case basing on the speciation in solution, 30% of the affected spectrum for KH_2PO_4 was subtracted from the affected spectrum for H_3PO_4 and likewise 30% of the affected spectrum for K_2HPO_4 was subtracted from the affected spectrum for K_3PO_4. Technically, the subtraction factor for a finite concentration is applied to affected spectra in the infinite dilution limit approximation. However, since the molar absorptivity derivative in Eq. (1) is based on finite concentration experimental spectra plus the bulk water spectrum, the true infinite dilution conditions are obtainable only if the $\varepsilon = f(m)$ relation can be safely extrapolated to very low concentrations. From our previous investigations it is apparent that the molar absorptivity derivative still carries some information about the finite concentration conditions (e.g., the common cation and anion influence on the water spectra).[23] Therefore, the subtraction conditions for the lowest concentration experimental spectrum seem to be a safe assumption.

The "artificial" spectra resulting from the above subtraction were again subjected to the fitting procedure. Eventually, the resulting component bands were found to differ no more than several cm^{-1} in position at maximum from the original ones (Table 1), with a single exception found for the 2301 cm^{-1} band for K_3PO_4 that became red shifted to 2280 cm^{-1}. This, however, does not influence the interpretation proposed above (Table 3). The details of this procedure are available as supporting information to this paper.

Further analysis may be enabled by transforming the molar absorptivity vibrational spectrum $\varepsilon_a(\nu_{OD})$ to the probability distribution of interatomic oxygen-oxygen distance $P(R_{OO})$. The details of this transformation were given elsewhere.[19,21] It is based on the generalization of the empirical relationship already used for transforming the average R_{OO} to ν^c_{OD}.[44] The obtained probability distributions are shown in Figure 9 and compared with bulk water. This graph once again illustrates the series of water "structure making" properties of the studied phosphates: $H_3PO_4 \approx KH_2PO_4 < K_2HPO_4 < K_3PO_4$. It is also apparent that the probability distribution becomes more structured and asymmetric along this series.

Another possibility for interpretation of the affected HDO spectra in terms of water "structure making" effects is offered by application of the Badger-Bauer rule,[52] which states that the average energy of water intermolecular interactions (ΔU_w) changes linearly with the stretching band frequency (ν^o_{OD}). The details of its formulation for HDO spectra were provided before[5] and it has been applied often for their interpretation.[5,42,43] The ΔU_w values for phosphates calculated basing on the bands attributed to P=O···H-OH and HO-H···OH_2 groupings are collected in Table 4. The application of the rule to H-bonds of the P-OH···OH_2 type is questionable, however, as the OD stretching frequency is not due to the water molecule vibrations. For the HO-H···OH_2 situation, $H_2PO_4^-$ and PO_4^{3-} are assumed to be identical to bulk water, basing on the PCM calculations (Table 2). In the same situation the calculated HDO band position is used for HPO_4^{2-} due to the experimental band having several concurrent interpretations. As it can be seen, ΔU_w(P=O···H-OH) rises quickly with increasing charge and for PO_4^{3-} is double the ΔU_w for bulk HDO. The previous observations about water structure in the hydration shell (HO-H···OH_2) are also confirmed from the energetic point of view.

Conclusions

The difference spectra method, which allows determination of the solute-affected water spectrum by removing the bulk water contribution from the spectra of solution series, may be coupled successfully with static ab initio (or DFT) calculations that aid in the interpretation of analytical component bands in the affected spectrum.

The phosphate family investigated in this work exhibits "structure making" properties in aqueous solution, but only for H_3PO_4 a real effect pertaining to water-water interactions can be observed. Nevertheless, all the phosphates are strongly hydrated, as evidenced fully by interatomic oxygen-

oxygen distance probability distributions, which maxima are strongly shifted towards lower distances from the bulk water position.

The interpretation of experimental bands and calculation results has been strengthened by showing simple linear relationships connecting the band position for a specific type of interaction with acidity or basicity of the solute. The principal HDO band related to anion hydration and attributed to P=O···H-OH type of H-bonds becomes red shifted with increasing basicity, while for P-OH···OH_2 type bonds increasing acidity causes the same effect. The appearance of the latter type of bonds in the affected spectra is a direct consequence of isotopic substitution with deuterium occurring on the phosphate anions and phosphoric acid.

Some earlier observations, specifically about potassium ion hydration and the appearance of shared "cation + anion" component band in the affected spectra have been independently confirmed in the present study. Also, the linear dependence of the anion-affected HDO band position on the polarizing power of the anion has been demonstrated, with the phosphates forming their own class of solutes.

The general observations presented here have direct far-reaching consequences, e.g. in the interpretation of hydration effects on phosphate linkages in nucleic acids and phosphate head groups in phospholipids.

Acknowledgments. This work was supported from the Republic of Poland scientific funds as a research project, within grant no. N N204 3799 33. Calculations were carried out at the Academic Computer Center in Gdańsk (TASK).

Supporting Information Available: Gas phase optimized structures of the phosphates' clusters in Cartesian coordinates; gas phase electronic energies and zero point energies of the clusters; derivation of equations allowing calculation of phosphate speciation in an aqueous solution; results of mutual subtraction of affected HDO spectra (spectra plots and band positions tables). This material is available free of charge via the Internet at http://pubs.acs.org.

References

(1) Saenger, W. *Principles of Nucleic Acid Structure*; Springer-Verlag: New York, 1984; pp 82-88.

(2) Baril, J.; Max, J.-J; Chapados, C. *Can. J. Chem.* **2000**, *78*, 490.

(3) Koeppen, B. M. *Adv. Physiol. Edu.* **1998**, *275*, 132.

(4) Lide, D. R., Ed. *CRC Handbook of Chemistry and Physics,* 88th Ed.; CRC Press: Boca Raton, FL, 2008; pp 8-40-8-41.

(5) Stangret, J.; Gampe T. *J. Phys. Chem. A* **2002**, *106*, 5393.

(6) Mason, P. E.; Cruickshank, J. M.; Neilson, G. W.; Buchanan, P. *Phys. Chem. Chem. Phys.* **2003**, *5*, 4686.

(7) Brandán, S. A.; Díaz, S. B.; González, J. J. L.; Disalvo, E. A.; Altabef, A. B. *Spectrochim. Acta A* **2007**, *66*, 884.

(8) Rudolph, W. W.; Irmer, G. *Appl. Spectrosc.* **2007**, *61*, 1312.

(9) Pribil, A. B.; Hofer, T. S.; Randolf, B. R.; Rode, B. M. *J. Comput. Chem.* **2008**, *29*, 2330.

(10) Ebner, C.; Onthong, U.; Probst, M. *J. Mol. Liquids* **2005**, *118*, 15.

(11) Zundel, G. In *The Hydrogen Bond - Recent Developments in Theory and Experiments*; Schuster, P.; Zundel, G.; Sandorfy, C., Eds.; North-Holland: Amsterdam, 1976; Vol. 2, pp 683-766.

(12) Schiöberg, D.; Hofmann, K. P.; Zundel, G. *Z. Phys. Chem. (Neue Folge)* **1974**, *90*, 181.

(13) Kameda, Y.; Sugawara, K.; Hosaka, T.; Usuki, T.; Uemura, O. *Bull. Chem. Soc. Japan* **2000**, *73*, 1105.

(14) Caminiti, R.; Cucca, P.; Atzei, D. *J. Phys. Chem.* **1985**, *89*, 1457.

(15) Waldron, R. D. *J. Chem. Phys.* **1957**, *26*, 809.

(16) Hornig, D. F. *J. Chem. Phys.* **1964**, *40*, 3119.

(17) Falk, M.; Ford, T. A. *Can. J. Chem.* **1966**, *44*, 1699.

(18) Kristiansson, O.; Lindgren, J.; de Villepin, J. *J. Phys. Chem.* **1988**, *92*, 2680.

(19) Kristiansson, O.; Eriksson, A.; Lindgren, J. *Acta Chem. Scand. A* **1984**, *38*, 613.

(20) Stangret, J. *Spectrosc. Lett.* **1988**, *21*, 369.

(21) Stangret, J.; Gampe, T. *J. Phys. Chem. B* **1999**, *103*, 3778.

(22) Preston, C. M.; Adams, W. A. *J. Phys. Chem.* **1979**, *83*, 814.

(23) Gojło, E.; Śmiechowski, M.; Stangret, J. *J. Phys. Chem. B* **2004**, *108*, 15938.

(24) Farr, T. D. *Phosphorus: Properties of the Element and Some of Its Compounds*, Tennessee Valley Authority, Chemical Engineering Report No. 8, U.S. Government Printing Office: Washington, D.C., 1950. Online version available from Innophos®. http://www.innophos.com/brochures/acid/page12.asp#table7 (accessed November 17, 2008).

(25) Pye, C. C.; Rudolph, W. W. *J. Phys. Chem. A* **2003**, *107*, 8746.

(26) Pye, C. C.; Michels, M. R. *Can. J. Anal. Sci. Spectrosc.* **2005**, *50*, 70.

(27) Pye, C. C.; Michels, M. R. *Can. J. Anal. Sci. Spectrosc.* **2004**, *49*, 175.

(28) Ruben, E. A.; Chapman, M. S.; Evanseck, J. D. *J. Phys. Chem. A* **2007**, *111*, 10804.

(29) Krishnan, R.; Binkley, J. S.; Seeger, R.; Pople, J.A. *J. Chem. Phys.* **1980**, *72*, 650.

(30) Frisch, M. J.; Pople, J. A.; Binkley, J. S. *J. Chem. Phys.* **1984**, *80*, 3265.

(31) Clark, T.; Chandrasekhar, J.; Spitznagel, G. W.; Schleyer, P. V. R. *J. Comput. Chem.* **1983**, *4*, 294.

(32) Becke, A. D. *J. Chem. Phys.* **1993**, *98*, 5648.

(33) Lee, C.; Yang, W.; Parr, R. G. *Phys. Rev. B* **1998**, *37*, 785.

(34) Peng, C.; Ayala, P. Y.; Schlegel, H. B.; Frisch, M. J. *J. Comp. Chem.* **1996**, *17*, 49.

(35) Cancès, M. T.; Mennucci, B.; Tomasi, J. *J. Chem. Phys.* **1997**, *107*, 3032.

(36) Mennucci, B.; Tomasi, J. *J. Chem. Phys.* **1997**, *106*, 5151.

(37) Cossi, M.; Scalmani, G.; Rega, N.; Barone, V. *J. Chem. Phys.* **2002**, *117*, 43.

(38) Csaszar, P.; Pulay, P. *J. Mol. Struct. (Theochem)* **1984**, *114*, 31.

(39) Gaussian 03, Revision C.02, Frisch, M. J.; Trucks, G. W.; Schlegel, H. B.; Scuseria, G. E.; Robb, M. A.; Cheeseman, J. R.; Montgomery, Jr., J. A.; Vreven, T.; Kudin, K. N.; Burant, J. C.; Millam, J. M.; Iyengar, S. S.; Tomasi, J.; Barone, V.; Mennucci, B.; Cossi, M.; Scalmani, G.; Rega, N.; Petersson, G. A.; Nakatsuji, H.; Hada, M.; Ehara, M.; Toyota, K.; Fukuda, R.; Hasegawa, J.; Ishida, M.; Nakajima, T.; Honda, Y.; Kitao, O.; Nakai, H.; Klene, M.; Li, X.; Knox, J. E.; Hratchian, H. P.; Cross, J. B.; Bakken, V.; Adamo, C.; Jaramillo, J.; Gomperts, R.; Stratmann, R. E.; Yazyev, O.; Austin, A. J.; Cammi, R.; Pomelli, C.; Ochterski, J. W.; Ayala, P. Y.; Morokuma, K.; Voth, G. A.; Salvador, P.; Dannenberg, J. J.; Zakrzewski, V. G.; Dapprich, S.; Daniels, A. D.; Strain, M. C.; Farkas, O.; Malick, D. K.; Rabuck, A. D.; Raghavachari, K.; Foresman, J. B.; Ortiz, J. V.; Cui, Q.; Baboul, A. G.; Clifford, S.; Cioslowski, J.; Stefanov, B. B.; Liu, G.; Liashenko, A.; Piskorz, P.; Komaromi, I.; Martin, R. L.; Fox, D. J.; Keith, T.; Al-Laham, M. A.; Peng, C. Y.; Nanayakkara, A.; Challacombe, M.; Gill, P. M. W.; Johnson, B.; Chen, W.; Wong, M. W.; Gonzalez, C.; Pople, J. A.; Gaussian, Inc.: Wallingford, CT, 2004.

(40) Marcus, Y. *Chem. Rev.* **1988**, *88*, 1475.

(41) Ohtaki, H.; Radnai, T. *Chem. Rev.* **1993**, *93*, 1157.

(42) Śmiechowski, M.; Stangret, J. *J. Phys. Chem. A* **2007**, *111*, 2889.

(43) Śmiechowski, M.; Stangret, J. *J. Chem. Phys.* **2006**, *125*, 204508.

(44) Berglund, B.; Lindgren, J.; Tegenfeldt, J. *J. Mol. Struct.* **1978**, *43*, 179.

(45) Klähn, M.; Mathias, G.; Kötting, C.; Nonella, M.; Schlitter, J.; Gerwert, K.; Tavan, P. *J. Phys. Chem. A* **2004**, *108*, 6186.

(46) Steger, E.; Herzog, K. *Z. Anorg. Allg. Chem.* **1964**, *331*, 169.

(47) Chapman, A. C.; Thirlwell, L. E. *Spectrochim. Acta* **1964**, *20*, 937.

(48) Chapman, A. C.; Long, D. A.; Jones, D. T. L. *Spectrochim. Acta* **1965**, *21*, 633.

(49) Deng, H.; Wang, J.; Callender, R.; Jay, W. J. *J. Phys. Chem. B* **1998**, *102*, 3617.

(50) Berglund, B.; Lindgren, J.; Tegenfeldt, J. *J. Mol. Struct.* **1978**, *43*, 169.

(51) Marcus, Y. *Ion Properties*; Marcel Dekker, Inc.: New York, 1997; pp 43-62.

(52) Badger, R. M.; Bauer, S. H. *J. Chem. Phys.* **1937**, *5*, 839.

Table 1. Selected Parameters of Analytical Bands from Decomposition of Spectra of HDO Affected by the Studied Phosphate Compounds

solute	ν^{o}_{OD} [a]	$\Delta_{½}$ [b]	I [c]	shape [d]
H_3PO_4	2625(3)	85	458	G
N = 13.9 [e]	2524(12)	152	4562	G
	2441(13)	183	3540	G×L
	2310(22)	294	2217	G
KH_2PO_4	2613(10)	91	733	G
N = 11.0 [e]	2550(13)	93	783	G
	2478(3)	182	6322	G
	2347(25)	316	4002	G
K_2HPO_4	2605(10)	85	394	G
N = 13.8 [e]	2546(11)	123	2344	G
	2440(20)	138	2278	G×L
	2363(22)	240	5364	G×L
K_3PO_4	2602(4)	110	1519	G
N = 16.2 [e]	2538(12)	79	916	G
	2434(11)	133	3203	G×L
	2301(10)	320	7071	G

[a] Band position at maximum (cm^{-1}), uncertainty of fit (as final digits of the value) given in parentheses. [b] Full-width at half-height (cm^{-1}). [c] Integrated intensity ($dm^{-3}\cdot mol^{-1}\cdot cm^{-2}$). [d] G – Gaussian band, L – Lorentzian band. [e] Affected number.

Table 2. Average Hydrogen Bond Lengths in Different Structural Situations for the Optimized Aqueous Phosphate Clusters

solute	assignment[a]	gas phase			PCM		
		m[b]	R_{OO}[c]	ν^c_{OD}[d]	m[b]	R_{OO}[c]	ν^c_{OD}[d]
H_3PO_4	P-OH···OH_2	9	2.616(56)	2208(111)	9	2.597(36)	2170(75)
	P=O···H-OH	9	2.818(89)	2483(77)	9	2.845(53)	2506(40)
	HO-H···OH_2	15	2.821(115)	2485(95)	17	2.792(77)	2458(76)
	P-O(H)···H-OH	6	2.974(94)	2590(44)	4	3.013(28)	2609(14)
$H_2PO_4^-$	P-OH···OH_2	6	2.765(62)	2429(66)	6	2.694(21)	2339(31)
	P=O···H-OH	15	2.796(110)	2462(115)	15	2.798(49)	2464(51)
	HO-H···OH_2	18	2.903(96)	2549(66)	17	2.842(56)	2504(48)
	P-O(H)···H-OH	4	2.923(140)	2562(76)	3	2.903(51)	2549(32)
HPO_4^{2-}	P-OH···OH_2	3	3.096(107)	2640(33)	1	2.782(-)	2447(-)
	P=O···H-OH	20	2.740(85)	2400(120)	20	2.745(45)	2406(59)
	HO-H···OH_2	18	2.984(56)	2595(29)	17	2.914(57)	2556(34)
	P-O(H)···H-OH	3	2.948(66)	2577(39)	1	2.892(-)	2542(-)
PO_4^{3-}	P=O···H-OH	20	2.665(83)	2295(141)	23	2.678(44)	2315(68)
	P=O···H-OH···O=P	6	2.791(140)	2457(121)	0	-	-
	HO-H···OH_2	15	3.040(64)	2620(26)	16	2.855(27)	2514(22)

[a] The hydrogen bond in question is marked by ellipsis; see text for details. [b] Total number of H-bonds of specific type in all clusters of a given solute. [c] Average intermolecular oxygen-oxygen distance (Å); standard deviation (as final digits of the value) given in parentheses, where possible. [d] OD stretching band position calculated from Eq. (2) (cm^{-1}); standard deviation given as for R_{OO}.

Table 3. Proposed Interpretation of Analytical Bands from Decomposition of Spectra of HDO Affected by the Studied Phosphate Compounds

solute	ν^{o}_{OD} [a]	interpretation [b]	color code [c]
H_3PO_4	2625	P-O(H)···H-OH	orange
	2524	P=O···H-OH	red
	2441	HO-H···OH_2 in the hydration sphere	black
	2310	P-OH···OH_2	blue
KH_2PO_4	2613	(K^+ + anion)-affected water	cyan
	2550	K^+-affected water; P-O(H)···H-OH	green
	2478	P=O···H-OH	red
	2347	P-OH···OH_2	blue
K_2HPO_4	2605	(K^+ + anion)-affected water	cyan
	2546	K^+-affected water; HO-H···OH_2 in anion hydration sphere; P-O(H)···H-OH	green
	2440	P-OH···OH_2	blue
	2363	P=O···H-OH	red
K_3PO_4	2602	(K^+ + anion)-affected water	cyan
	2538	K^+-affected water	green
	2434	"Double donor" H_2O; P-OH···OH_2 of HPO_4^{2-}	magenta
	2301	P=O···H-OH	red

[a] Band position at maximum (cm^{-1}). [b] H-bond type assigned to specific analytical band (see text for details). [c] Color used to designate specific band types in Figure 4.

Table 4. Intermolecular Interaction Energy of Water Estimated from the Phosphate-Affected HDO Spectra Component Bands' Positions

solute	ΔU_w (P=O···H-OH)[a]	ΔU_w (HO-H···OH_2)[a]
H_3PO_4	-38.5	-55.4
KH_2PO_4	-47.9	-41.5[b]
K_2HPO_4	-71.3	-31.9[c]
K_3PO_4	-84.0	-41.5[b]
HDO	-	-41.5

[a] Intermolecular interaction energy of water in the indicated molecular situation (kJ·mol^{-1}), estimated from ν^o_{OD} (Table 1). [b] ν^o_{OD} assumed equal to bulk HDO (see Table 2). [c] Based on ν^c_{OD} (see Table 2).

Figure 1. Relative concentrations of different phosphate(V) forms dependent on the pH of aqueous solutions: H_3PO_4 (solid line), KH_2PO_4 (dashed line), K_2HPO_4 (dotted line), K_3PO_4 (dashed-dotted line). Shaded regions represent pH ranges in which pH of the studied solutions is expected, with solute names given above for reference.

Figure 2. Experimental FT-IR spectra of HDO in the OD stretching range of aqueous solutions of: (a) H_3PO_4, (b) KH_2PO_4, (c) K_2HPO_4 and (d) K_3PO_4 (solid lines, left axis) and the corresponding derivatives at infinite dilution limit $(\partial\varepsilon/\partial m)_{m=0}$ (dashed lines, right axis).

Figure 3. (a) Derivatives at infinite dilution limit $(\partial\varepsilon/\partial m)_{m=0}$, (b) corresponding affected spectra and (c) second derivatives of the affected spectra for H_3PO_4 (blue), KH_2PO_4 (green), K_2HPO_4 (orange) and K_3PO_4 (red). Bulk HDO spectrum is shown in subfigure (b) for comparison (black). Open circles in subfigure (c) denote the minima.

Figure 4. Solute-affected HDO spectra for (a) H_3PO_4, (b) KH_2PO_4, (c) K_2HPO_4 and (d) K_3PO_4 aqueous solutions (solid lines) and decomposition into analytical component bands (dashed lines, colored according to common interpretation, see Table 3).

Figure 5. Aqueous phosphate clusters, $X(H_2O)_n$ ($X = H_3PO_4$, $H_2PO_4^-$, HPO_4^{2-}, PO_4^{3-}; n = 7–9) studied in this work, in their B3LYP/6-311++G(d,p) gas-phase optimized geometries. Black spheres denote phosphorus, red spheres – oxygens, gray spheres – hydrogens. Hydrogen bonds indicated by dashed lines.

Figure 6. Dependence of (a) ν^c_{OD} for the P-OH···OH_2 grouping on pK_a of the solute, (b) ν^c_{OD} for the P=O···H-OH grouping on pK_b of the solute. Symbols indicate gas phase (open circles + solid line, linear fit) and PCM (open squares + dashed line, linear fit) calculations and the corresponding analytical component bands in experimental solute-affected spectra (solid diamonds). Error bars correspond to uncertainty of fit and standard deviations of ν^c_{OD}. Solute formulae are given above the points for quick reference.

Figure 7. Dependence of ν^o_{OD} for the principal anion-affected HDO band on the polarizing power of the anion. Error bars correspond to uncertainty of fit. Solid line shows the linear least-squares fit of data for

the phosphate(V) anions studied in this work. The correlations found previously are shown as dashed lines. Data for other anions were collected and discussed in Ref. 5.

Figure 8. Dependence of ν^{o}_{OD} for the "cation+anion" component band in the affected HDO spectra on ν^{o}_{OD} for the principal anion-affected HDO band. Error bars correspond to uncertainty of fit. Solid line shows the linear least-squares fit of data.

Figure 9. Interatomic oxygen-oxygen distance distribution derived from the affected HDO spectra shown in Fig. 3(b) for: H_3PO_4 (blue), KH_2PO_4 (green), K_2HPO_4 (orange), K_3PO_4 (red) and bulk HDO (black).

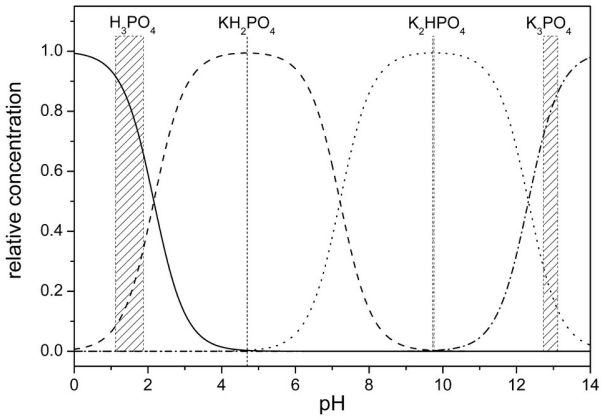

Figure 1. Relative concentrations of different phosphate(V) forms dependent on the pH of aqueous solutions: H_3PO_4 (solid line), KH_2PO_4 (dashed line), K_2HPO_4 (dotted line), K_3PO_4 (dashed-dotted line). Shaded regions represent pH ranges in which pH of the studied solutions is expected, with solute names given above for reference.

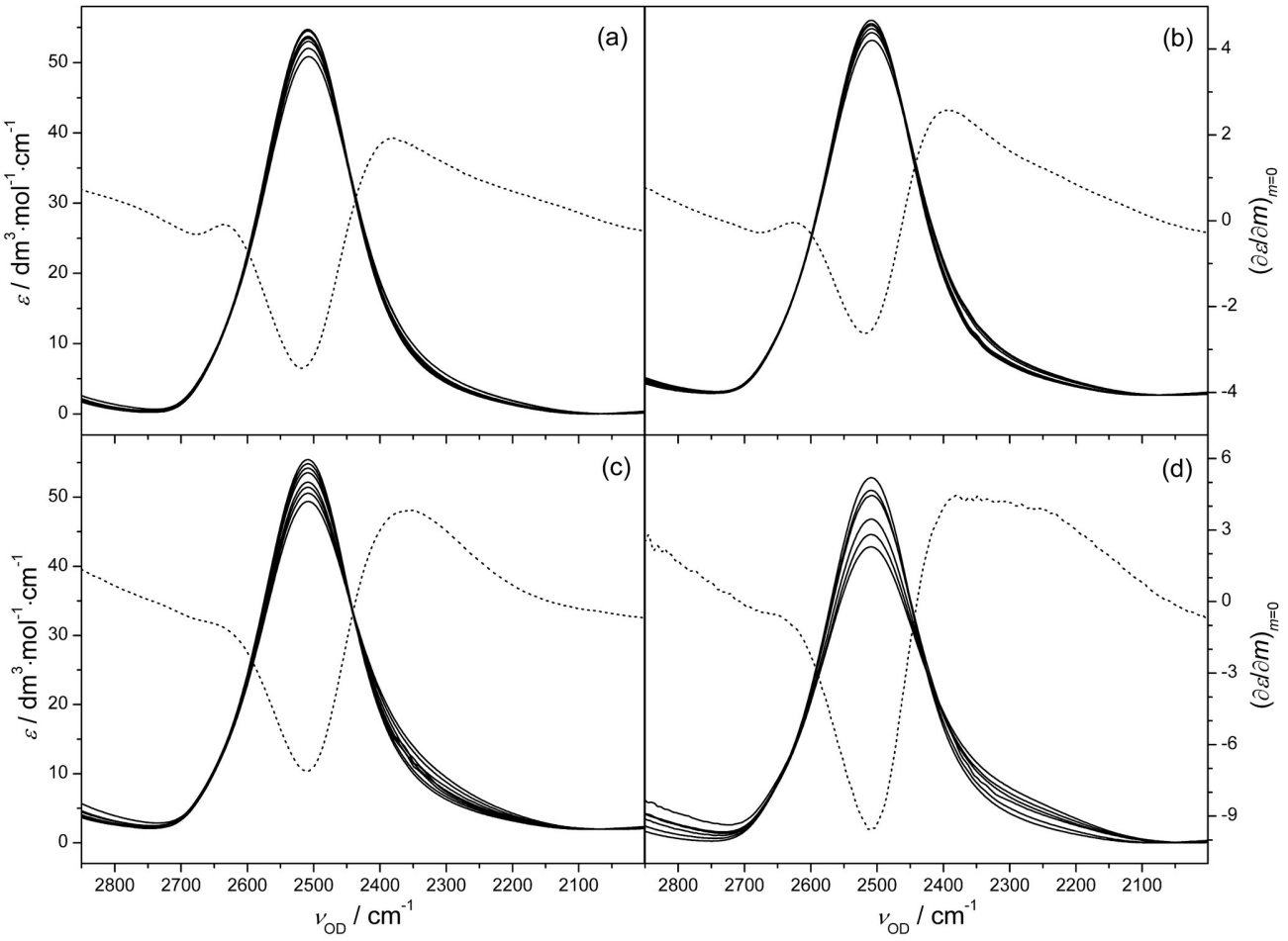

Figure 2. Experimental FT-IR spectra of HDO in the OD stretching range of aqueous solutions of: (a) H_3PO_4, (b) KH_2PO_4, (c) K_2HPO_4 and (d) K_3PO_4 (solid lines, left axis) and the corresponding derivatives at infinite dilution limit $(\partial\varepsilon/\partial m)_{m=0}$ (dashed lines, right axis).

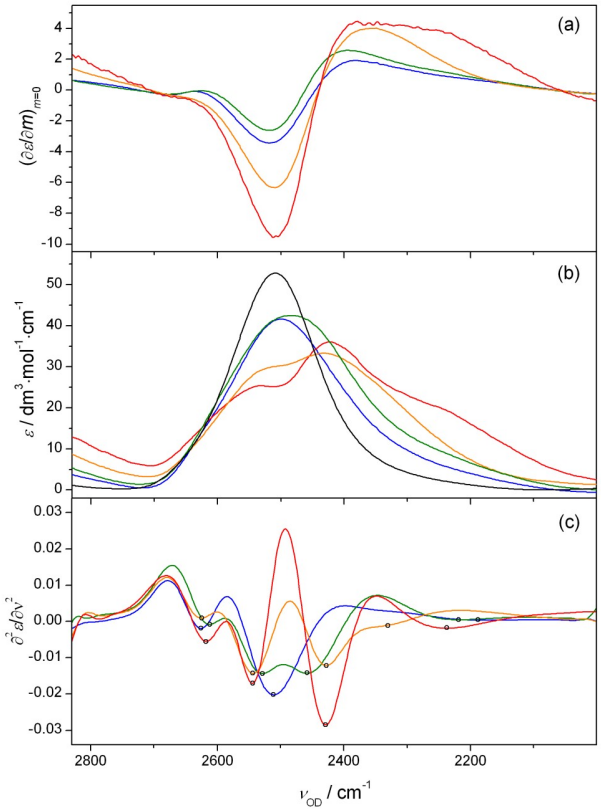

Figure 3. (a) Derivatives at infinite dilution limit $(\partial\varepsilon/\partial m)_{m=0}$, (b) corresponding affected spectra and (c) second derivatives of the affected spectra for H_3PO_4 (blue), KH_2PO_4 (green), K_2HPO_4 (orange) and K_3PO_4 (red). Bulk HDO spectrum is shown in subfigure (b) for comparison (black). Open circles in subfigure (c) denote the minima.

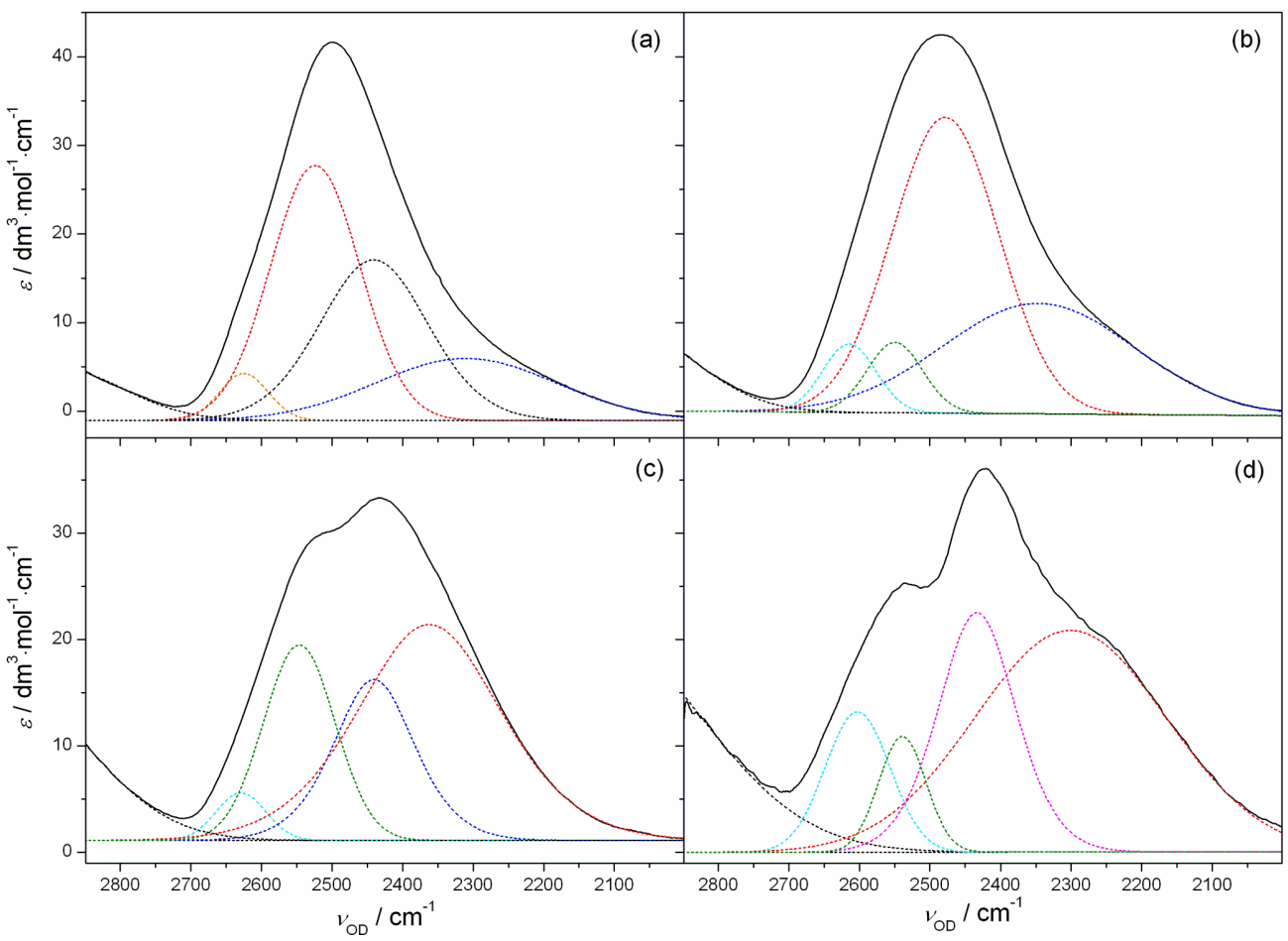

Figure 4. Solute-affected HDO spectra for (a) H_3PO_4, (b) KH_2PO_4, (c) K_2HPO_4 and (d) K_3PO_4 aqueous solutions (solid lines) and decomposition into analytical component bands (dashed lines, colored according to common interpretation, see Table 3).

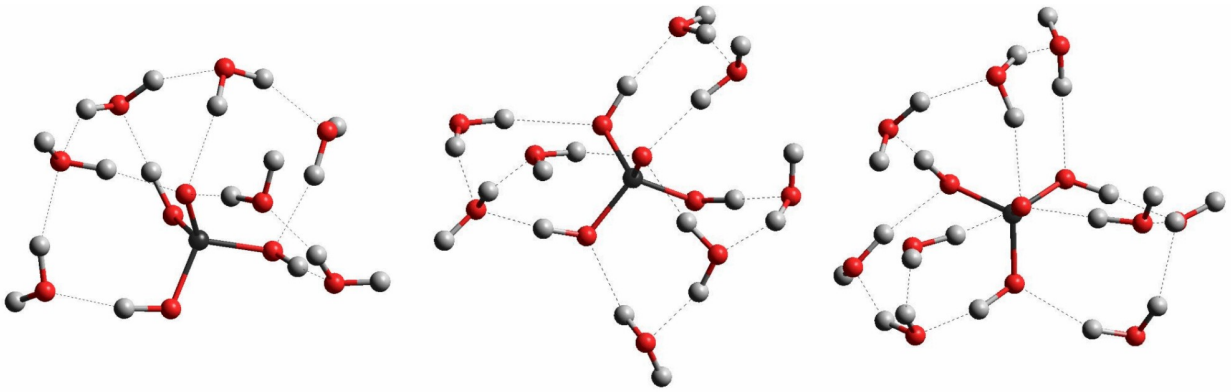

$H_3PO_4(H_2O)_7$ $H_3PO_4(H_2O)_8$ $H_3PO_4(H_2O)_9$

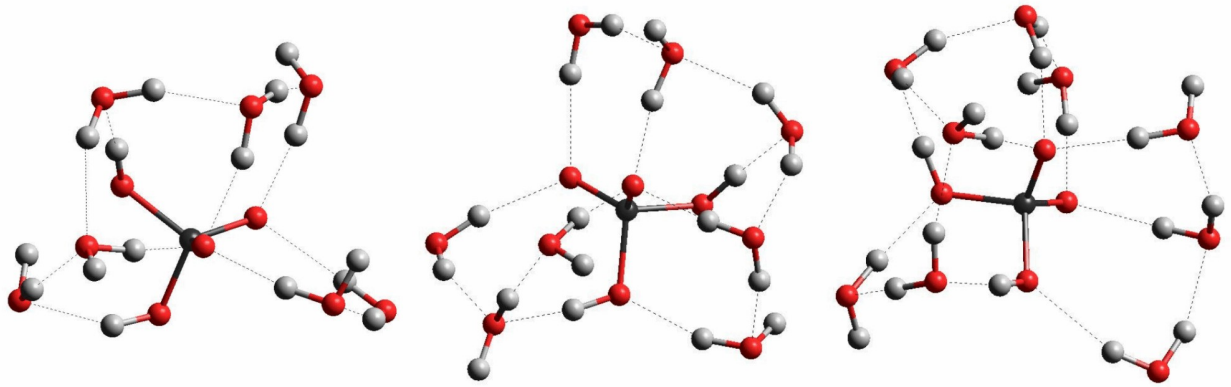

$H_2PO_4^-(H_2O)_7$ $H_2PO_4^-(H_2O)_8$ $H_2PO_4^-(H_2O)_9$

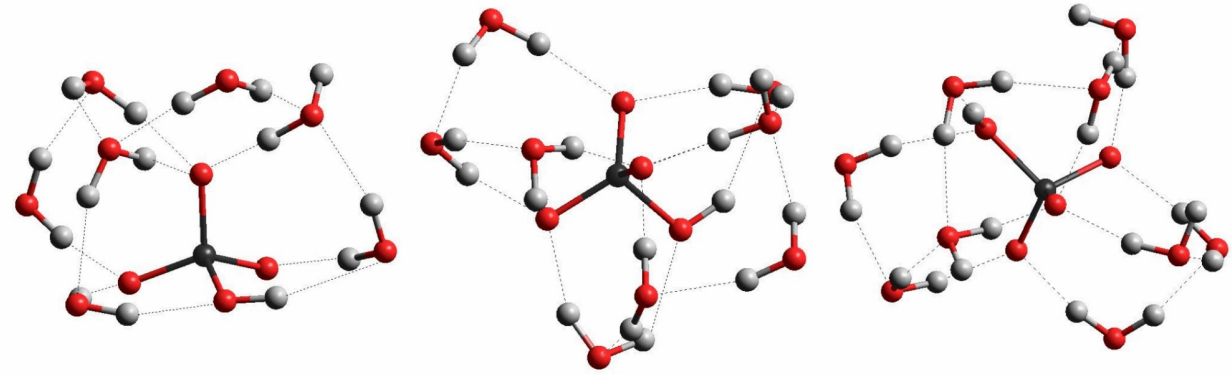

$HPO_4^{2-}(H_2O)_7$ $HPO_4^{2-}(H_2O)_8$ $HPO_4^{2-}(H_2O)_9$

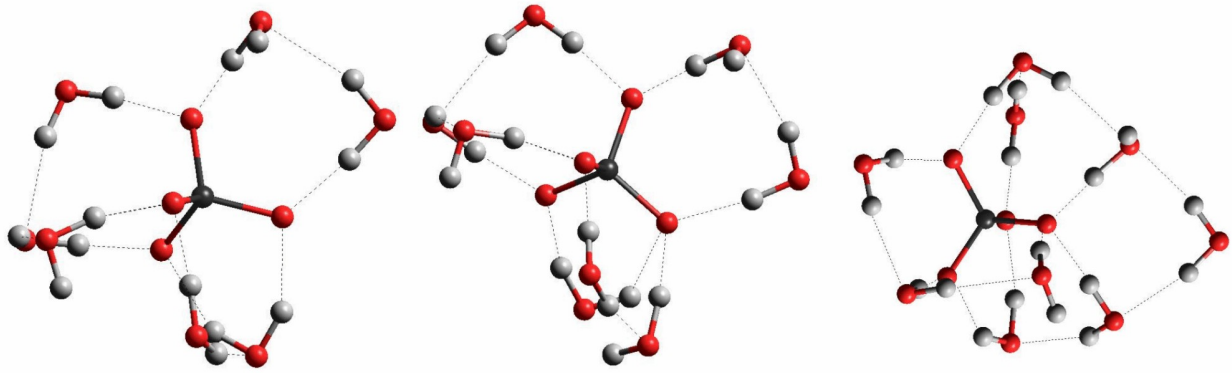

$PO_4^{3-}(H_2O)_7$ $PO_4^{3-}(H_2O)_8$ $PO_4^{3-}(H_2O)_9$

Figure 5. Aqueous phosphate clusters, $X(H_2O)_n$ ($X = H_3PO_4$, $H_2PO_4^-$, HPO_4^{2-}, PO_4^{3-}; n = 7–9) studied in this work, in their B3LYP/6-311++G(d,p) gas-phase optimized geometries. Black spheres denote phosphorus, red spheres – oxygens, gray spheres – hydrogens. Hydrogen bonds indicated by dashed lines.

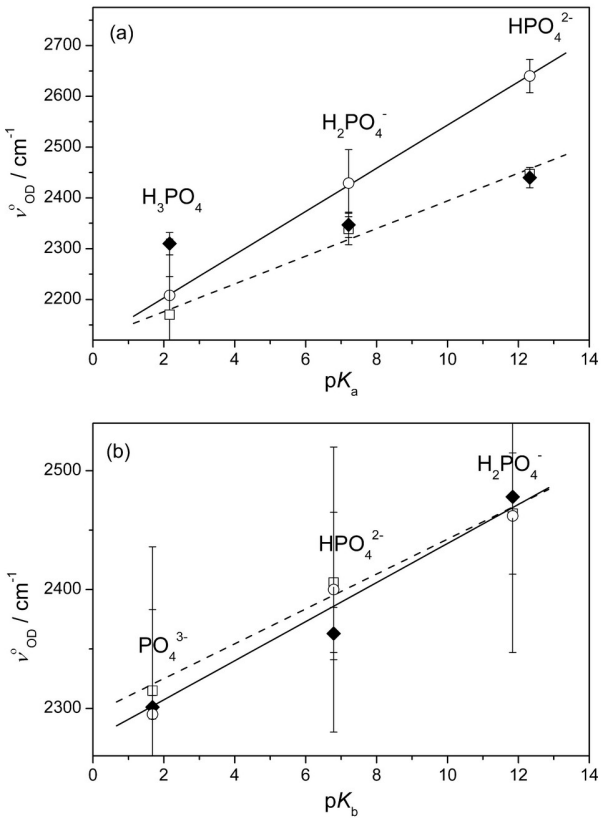

Figure 6. Dependence of (a) ν^{c}_{OD} for the P-OH···OH_2 grouping on pK_a of the solute, (b) ν^{c}_{OD} for the P=O···H-OH grouping on pK_b of the solute. Symbols indicate gas phase (open circles + solid line, linear fit) and PCM (open squares + dashed line, linear fit) calculations and the corresponding analytical component bands in experimental solute-affected spectra (solid diamonds). Error bars correspond to uncertainty of fit and standard deviations of ν^{c}_{OD}. Solute formulae are given above the points for quick reference.

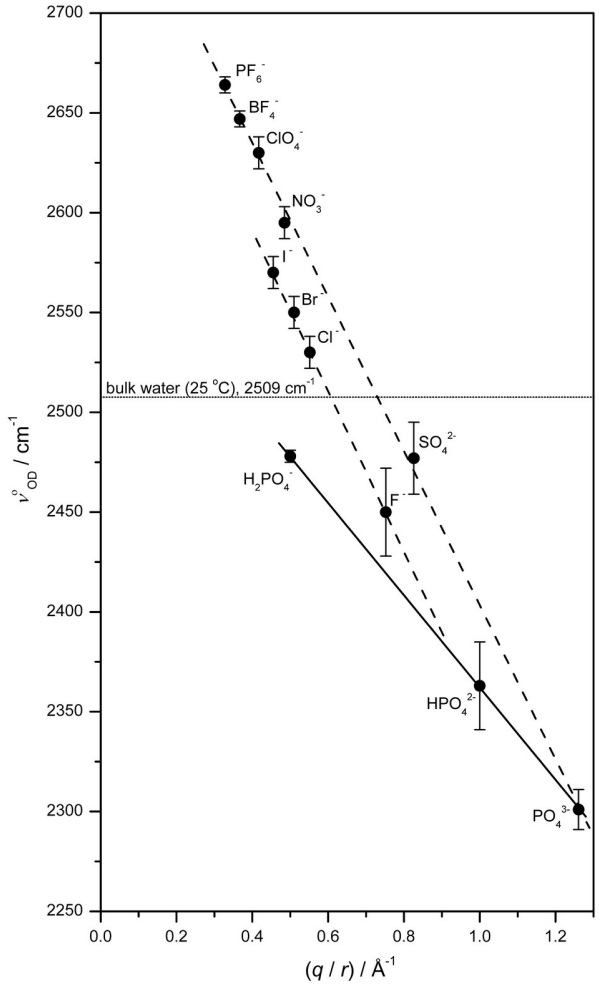

Figure 7. Dependence of ν^{o}_{OD} for the principal anion-affected HDO band on the polarizing power of the anion. Error bars correspond to uncertainty of fit. Solid line shows the linear least-squares fit of data for the phosphate(V) anions studied in this work. The correlations found previously are shown as dashed lines. Data for other anions were collected and discussed in Ref. 5.

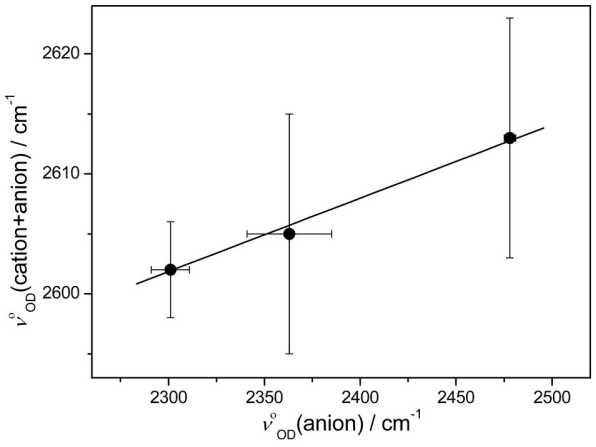

Figure 8. Dependence of ν^{o}_{OD} for the "cation+anion" component band in the affected HDO spectra on ν^{o}_{OD} for the principal anion-affected HDO band. Error bars correspond to uncertainty of fit. Solid line shows the linear least-squares fit of data.

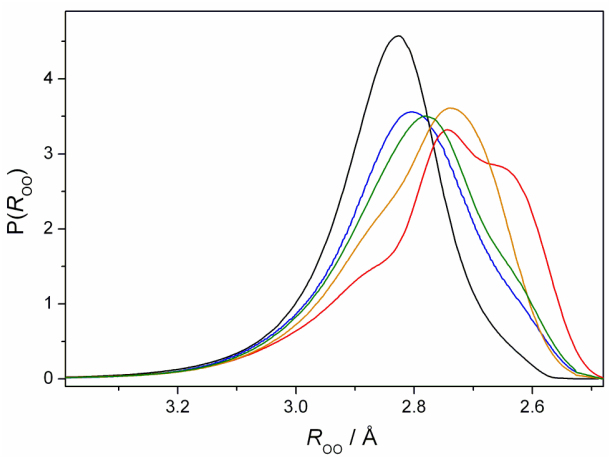

Figure 9. Interatomic oxygen-oxygen distance distribution derived from the affected HDO spectra shown in Fig. 3(b) for: H_3PO_4 (blue), KH_2PO_4 (green), K_2HPO_4 (orange), K_3PO_4 (red) and bulk HDO (black).

Systematic Study of Hydration Patterns of Phosphoric(V) Acid and Its Mono-, Di-, and Tripotassium Salts in Aqueous Solution

Maciej Śmiechowski, Emilia Gojło, and Janusz Stangret*

Department of Physical Chemistry, Chemical Faculty, Gdańsk University of Technology, Narutowicza 11/12, 80-952 Gdańsk, Poland

* To whom correspondence should be addressed. Phone: (+48) 58 347 1283. Fax: (+48) 58 347 2694. E-mail address: msmiech@chem.pg.gda.pl.

Supporting Information

Tables S1-S12. Optimized Gas Phase Structures of $X(H_2O)_n$ (X = H_3PO_4, $H_2PO_4^-$, HPO_4^{2-}, PO_4^{3-}; n = 7–9) at the B3LYP/6-311++G(d,p) Level of Theory in Cartesian Coordinates

Table S13. Gas Phase Electronic Energies and Zero Point Energies of $X(H_2O)_n$ (X = H_3PO_4, $H_2PO_4^-$, HPO_4^{2-}, PO_4^{3-}; n = 7–9) at the B3LYP/6-311++G(d,p) Level of Theory

Composition of Aqueous Phosphate Solutions – Derivation of Formal Equations.

Figure S1. Affected HDO spectrum obtained by subtracting 30% of the original affected HDO spectrum for KH_2PO_4 from the original affected HDO spectrum for H_3PO_4 (solid line) and its decomposition into analytical component bands (dashed lines).

Table S14. Selected Parameters of Analytical Bands from Decomposition of the HDO Spectrum shown in Fig. S1.

Figure S2. Affected HDO spectrum obtained by subtracting 30% of the original affected HDO spectrum for K_2HPO_4 from the original affected HDO spectrum for K_3PO_4 (solid line) and its decomposition into analytical component bands (dashed lines).

Table S15. Selected Parameters of Analytical Bands from Decomposition of the HDO Spectrum shown in Fig. S2.

Table S1. Optimized Gas Phase Structure of $H_3PO_4(H_2O)_7$ at the B3LYP/6-311++G(d,p) Level

Atom	X / Å	Y / Å	Z / Å
P	-0.026791	-0.429893	-0.749315
O	-0.149445	-0.229408	0.757724
O	-0.769270	0.681620	-1.573931
H	-1.233521	1.412460	-1.037153
O	-0.551459	-1.841766	-1.228568
H	-1.492901	-2.013681	-0.960655
O	1.475008	-0.359186	-1.257989
H	2.115932	-1.003152	-0.822178
O	3.076922	-1.946180	0.062147
H	2.798503	-1.838080	1.000314
H	4.034550	-1.867539	0.029605
O	-1.903385	2.474319	-0.099378
H	-1.135124	2.758214	0.447283
H	-2.484507	1.988328	0.505401
O	-3.105093	-1.986364	-0.370333
H	-3.205013	-1.288576	0.308410
H	-3.820933	-1.864320	-1.001570
O	-2.747752	0.080371	1.492843
H	-1.773742	-0.054074	1.414648
H	-2.972888	-0.024048	2.422843
O	0.485729	2.583603	1.262513
H	0.418667	1.616322	1.317192
H	1.215629	2.723083	0.631090
O	1.775834	-1.406395	2.382913
H	1.016454	-0.986145	1.926782
H	2.039659	-0.803638	3.084344

Table S1. Continued

Atom	X / Å	Y / Å	Z / Å
O	2.436845	2.358481	-0.833737
H	2.201042	1.482030	-1.180758
H	2.488593	2.938444	-1.599517

Table S2. Optimized Gas Phase Structure of $H_3PO_4(H_2O)_8$ at the B3LYP/6-311++G(d,p) Level

Atom	X / Å	Y / Å	Z / Å
P	-0.155932	-0.139421	-0.593548
O	-0.206863	0.210474	0.887719
O	-0.889321	0.901796	-1.503747
H	-1.317178	1.704740	-1.033194
O	-0.747404	-1.580445	-0.899379
H	-1.689683	-1.682325	-0.585769
O	1.326699	-0.191005	-1.165209
H	1.931231	-0.857545	-0.727848
O	2.806189	-1.915170	0.205185
H	2.604708	-1.664383	1.139124
H	3.762287	-1.979467	0.115543
O	-1.908999	2.868310	-0.210303
H	-1.114843	3.184976	0.279884
H	-2.490621	2.479510	0.460650
O	-3.246473	-1.544621	0.040816
H	-3.316506	-0.774290	0.640280
H	-3.994550	-1.502173	-0.562856
O	-2.780322	0.694333	1.661267
H	-1.814276	0.518433	1.584665
H	-2.992719	0.699862	2.600209
O	0.514838	3.055112	1.063193
H	0.433948	2.105645	1.247009
H	1.236427	3.096902	0.408578
O	1.733203	-0.981741	2.489386
H	0.980938	-0.523548	2.059268
H	2.094253	-0.372867	3.140279

Table S2. Continued

Atom	X / Å	Y / Å	Z / Å
O	2.427403	2.518099	-1.005234
H	2.153908	1.629775	-1.285446
H	2.556535	3.022634	-1.814105
O	1.119160	-4.038070	-1.171596
H	0.383571	-3.422349	-1.275427
H	1.746680	-3.548813	-0.624405

Table S3. Optimized Gas Phase Structure of $H_3PO_4(H_2O)_9$ at the B3LYP/6-311++G(d,p) Level

Atom	X / Å	Y / Å	Z / Å
P	-0.242946	0.018267	-0.299629
O	0.367598	-0.094418	1.087810
O	0.849067	0.090866	-1.438743
H	1.835851	-0.038989	-1.129885
O	-1.192903	1.268193	-0.468223
H	-0.691320	2.149528	-0.358998
O	-1.135214	-1.241983	-0.683976
H	-1.919955	-1.403591	-0.082961
O	-3.078263	-1.567230	1.087974
H	-2.604534	-1.466569	1.948990
H	-3.622953	-2.358912	1.140722
O	3.217193	-0.166713	-0.601858
H	3.160835	-0.972441	-0.033950
H	3.334820	0.580505	0.007128
O	0.349162	3.344072	-0.329804
H	1.101458	3.120300	0.245574
H	0.700972	3.347140	-1.242595
O	2.283145	1.891649	1.308672
H	1.606087	1.200901	1.473371
H	2.601230	2.185621	2.168280
O	2.379930	-2.218869	0.985952
H	1.665466	-1.633951	1.286026
H	1.916121	-2.884442	0.445256
O	-1.364837	-0.986551	3.077626
H	-0.658364	-0.624297	2.503163
H	-0.935017	-1.544254	3.732409

Table S3. Continued

O	0.546676	-3.630958	-0.701541
H	-0.089240	-2.927820	-0.910591
H	0.717527	-4.092655	-1.527912
O	-4.253214	0.890168	-0.279006
H	-3.375492	1.231758	-0.489683
H	-4.070809	0.138588	0.298998
O	1.173853	2.585155	-2.863796
H	1.007318	1.645305	-2.685694
H	0.826653	2.767223	-3.741913

Table S4. Optimized Gas Phase Structure of $H_2PO_4^-(H_2O)_7$ at the B3LYP6-311++G(d,p) Level

Atom	X / Å	Y / Å	Z / Å
P	0.027041	-0.531316	-0.742634
O	-0.180269	-0.291875	0.772256
O	-1.079924	0.386435	-1.519106
H	-1.337841	1.204929	-1.023917
O	-0.455160	-2.014444	-1.150232
H	-1.409457	-2.134435	-0.972273
O	1.425740	-0.312818	-1.253590
H	2.926680	-1.426485	-0.459614
O	3.523690	-1.889793	0.151445
H	3.062778	-1.817423	1.001246
O	-1.939250	2.460751	0.059963
H	-1.097267	2.678765	0.517177
H	-2.409641	1.887882	0.687013
O	-3.255353	-1.509603	-0.806946
H	-3.279348	-1.094298	0.074443
H	-2.953270	-0.788272	-1.378494
O	-2.667344	0.023500	1.562005
H	-1.700463	-0.149081	1.358799
H	-2.789706	-0.187791	2.491681
O	0.579178	2.427219	1.254648
H	0.416838	1.463923	1.257094
H	1.268442	2.532133	0.568867
O	1.825781	-1.112856	2.525463
H	1.077621	-0.895445	1.927819
H	2.237352	-0.261357	2.702997

Table S4. Continued

Atom	X / Å	Y / Å	Z / Å
O	2.382908	2.213730	-0.940399
H	2.142725	1.265145	-1.089970
H	2.158945	2.649576	-1.767402

Table S5. Optimized Gas Phase Structure of $H_2PO_4^-(H_2O)_8$ at the B3LYP/6-311++G(d,p) Level

Atom	X / Å	Y / Å	Z / Å
P	-0.170325	0.191399	-0.654329
O	0.359451	0.075089	0.800668
O	1.052380	-0.106441	-1.656834
H	1.948999	-0.036521	-1.238724
O	-0.940096	1.432812	-0.989071
O	-1.060425	-1.155979	-0.956988
H	-1.932613	-1.134544	-0.511643
O	-3.262694	-1.067968	0.785890
H	-2.688787	-1.028162	1.589089
H	-3.890874	-1.781926	0.923805
O	3.454715	-0.092003	-0.346486
H	3.245288	-0.872247	0.204920
H	3.358839	0.663196	0.259644
O	0.601001	3.870213	-0.340730
H	1.255091	3.379632	0.175200
H	-0.016467	3.178054	-0.636434
O	2.259131	1.887933	1.361568
H	1.490677	1.266899	1.270687
H	2.277901	2.160180	2.283013
O	2.088433	-2.126238	1.107320
H	1.438104	-1.393158	1.112736
H	1.738856	-2.722724	0.421292
O	-1.328687	-0.822403	2.687799
H	-0.692427	-0.403476	2.048532
H	-0.870150	-1.609622	2.997625

Table S5. Continued

Atom	X / Å	Y / Å	Z / Å
O	0.772346	-3.292504	-1.239218
H	0.007417	-2.691757	-1.149172
H	1.295545	-2.854134	-1.919917
O	-3.832489	1.479256	-0.817518
H	-2.882656	1.621310	-0.982992
H	-3.832394	0.733888	-0.203933

Table S6. Optimized Gas Phase Structure of $H_2PO_4^-(H_2O)_9$ at the B3LYP/6-311++G(d,p) Level

Atom	X / Å	Y / Å	Z / Å
P	0.118286	-0.178528	-0.419408
O	0.009577	0.481950	0.971100
O	-1.306110	0.075235	-1.184476
H	-1.829394	0.846819	-0.827075
O	0.142373	-1.782816	-0.277218
H	-0.612497	-2.122381	0.269588
O	1.282950	0.252939	-1.272021
H	3.043420	-0.242414	-0.623279
O	3.775918	-0.535623	-0.050369
H	3.537612	-0.161548	0.814392
O	-2.709569	2.060407	-0.031194
H	-1.982180	2.693260	0.159207
H	-2.873940	1.611658	0.814256
O	-2.188756	-2.462268	0.996675
H	-2.421014	-1.658928	1.495901
H	-2.711901	-2.425372	0.174308
O	-2.308497	0.173526	2.207192
H	-1.383269	0.287756	1.848217
H	-2.244145	0.290857	3.159381
O	-0.271766	3.286418	0.536761
H	-0.051555	2.385115	0.841577
H	0.266769	3.378894	-0.273493
O	2.487333	0.837920	2.239688
H	1.595956	0.661344	1.869762
H	2.626670	1.776787	2.081720

Table S6. Continued

O	1.342034	2.930465	-1.794004
H	1.411363	1.952836	-1.662509
H	0.976310	3.031362	-2.677182
O	2.851918	-3.285944	-0.243610
H	1.936469	-2.983250	-0.311110
H	3.341661	-2.449755	-0.143164
O	-3.030968	-2.060599	-1.697302
H	-2.440106	-1.280015	-1.664854
H	-2.572023	-2.687983	-2.264304

Table S7. Optimized Gas Phase Structure of $HPO_4^{2-}(H_2O)_7$ at the B3LYP/6-311++G(d,p) Level

Atom	X / Å	Y / Å	Z / Å
P	-0.248309	-1.225653	0.040416
O	0.168789	0.126161	-0.670194
O	0.568674	-1.153028	1.529624
H	1.484149	-1.432112	1.388644
O	0.314516	-2.445471	-0.677639
O	-1.720200	-1.193665	0.453510
H	-3.148539	-0.672062	-0.594671
O	-3.801902	-0.222742	-1.176531
H	-3.262624	0.488282	-1.558248
O	2.442224	3.186514	0.418676
H	1.507692	3.056646	0.665469
H	2.646971	2.372660	-0.074198
O	3.027566	-2.217102	-0.249505
H	3.111403	-1.301678	-0.562158
H	2.095585	-2.447384	-0.495902
O	2.649431	0.643867	-1.126419
H	1.665088	0.416651	-0.954325
H	2.691683	0.766706	-2.078987
O	-0.354928	2.379943	0.768823
H	-0.125498	1.557438	0.260727
H	-0.805929	2.004272	1.545409
O	-1.654586	1.734251	-1.973507
H	-1.019906	1.032355	-1.690467
H	-1.600894	2.332854	-1.215757
O	-1.514990	0.442875	2.708983
H	-1.872923	-0.073079	1.947831
H	-0.638388	0.030426	2.763815

Table S8. Optimized Gas Phase Structure of $HPO_4^{2-}(H_2O)_8$ at the B3LYP/6-311++G(d,p) Level

Atom	X / Å	Y / Å	Z / Å
P	0.551362	0.396904	0.623431
O	-0.371892	-0.014374	-0.589134
O	-0.525151	0.795852	1.851393
H	-0.849264	1.697154	1.697261
O	1.346749	1.668173	0.318383
O	1.303345	-0.817401	1.174455
O	3.141282	-1.757539	-0.667119
H	2.471962	-1.895453	-1.357693
H	2.582619	-1.477985	0.097283
O	-4.256832	-0.487921	-1.017494
H	-3.637115	-1.146224	-0.650600
H	-3.687750	0.286135	-1.166324
O	-0.753114	3.491358	0.412424
H	-1.311297	3.060676	-0.256186
H	0.113057	3.026956	0.316945
O	-2.163547	1.626410	-1.470111
H	-1.445567	0.987864	-1.128114
H	-1.938573	1.749979	-2.396767
O	-2.024515	-2.147484	-0.099008
H	-1.435773	-1.377284	-0.301129
H	-1.774902	-2.343797	0.820630
O	0.614472	-1.901540	-2.298069
H	0.333259	-1.111693	-1.769173
H	0.067978	-2.593425	-1.908159
O	-0.718082	-2.063225	2.585628
H	0.127166	-1.840479	2.123109
H	-1.056236	-1.167036	2.727565

Table S8. Continued

Atom	X / Å	Y / Å	Z / Å
O	3.938051	1.173112	-0.817941
H	3.088926	1.460519	-0.420647
H	3.834952	0.207155	-0.846729

Table S9. Optimized Gas Phase Structure of $HPO_4^{2-}(H_2O)_9$ at the B3LYP/6-311++G(d,p) Level

Atom	X / Å	Y / Å	Z / Å
P	0.161494	-0.332667	-0.446424
O	0.119486	0.457035	0.923355
O	-1.166899	0.267733	-1.277359
H	-1.608496	0.991039	-0.795178
O	-0.061819	-1.828625	-0.275902
O	1.400390	0.075665	-1.261888
H	2.983006	-0.499704	-0.618905
O	3.741944	-0.794988	-0.061397
H	3.525079	-0.398427	0.797616
O	-2.423920	2.488559	0.317111
H	-1.542021	2.901388	0.406686
H	-2.486585	1.884139	1.076339
O	-2.482111	-2.396967	0.908984
H	-2.532907	-1.592715	1.447704
H	-1.584550	-2.322463	0.495910
O	-2.068066	0.326140	2.294039
H	-1.178938	0.320474	1.799165
H	-1.830753	0.339832	3.225021
O	0.363498	3.159746	0.469829
H	0.359222	2.199767	0.707056
H	0.692193	3.144612	-0.449621
O	2.500229	0.772315	2.220324
H	1.624841	0.536949	1.817260
H	2.640818	1.665392	1.888801
O	1.137708	2.518820	-2.266160
H	1.354208	1.598489	-1.927024
H	0.266981	2.377223	-2.653127

Table S9. Continued

Atom	X / Å	Y / Å	Z / Å
O	2.317205	-3.453994	-0.046296
H	1.447368	-3.015740	-0.147382
H	2.926446	-2.697372	-0.033294
O	-3.546303	-1.533054	-1.665908
H	-2.767256	-0.961473	-1.767479
H	-3.361794	-1.948477	-0.803048

Table S10. Optimized Gas Phase Structure of $PO_4^{3-}(H_2O)_7$ at the B3LYP/6-311++G(d,p) Level

Atom	X / Å	Y / Å	Z / Å
P	-0.246572	0.168643	0.179279
O	-1.808157	0.255206	0.331871
O	0.316254	-0.854465	1.241665
O	0.420518	1.586513	0.385021
O	0.104505	-0.368277	-1.275929
H	-2.387226	3.066889	-0.301752
O	-3.167584	2.546655	-0.049069
H	-2.730500	1.654123	0.120103
H	3.103118	0.637277	1.393726
O	2.984761	1.602359	1.424807
H	2.055986	1.684423	1.070744
O	2.865138	-1.436845	1.128737
H	1.874014	-1.220949	1.254646
H	2.886226	-1.571269	0.166751
H	-0.580231	2.992116	-1.846245
O	-0.449354	3.513074	-1.046870
H	-0.076000	2.767367	-0.412581
H	-2.279999	-1.413250	0.915934
O	-2.030462	-2.309533	1.264420
H	-1.087248	-2.064675	1.442824
H	-0.722179	-1.867059	-1.632149
O	-1.129033	-2.783030	-1.667462
H	-1.497774	-2.837022	-0.769181
H	1.625304	-2.626143	-1.720514
O	2.154173	-1.827506	-1.832523
H	1.429011	-1.124679	-1.608832

Table S11. Optimized Gas Phase Structure of $PO_4^{3-}(H_2O)_8$ at the B3LYP/6-311++G(d,p) Level

Atom	X / Å	Y / Å	Z / Å
P	0.079022	0.184665	0.055313
O	-1.314680	0.742053	0.558002
O	0.682619	-0.755852	1.167761
O	1.065142	1.380124	-0.220540
O	-0.140432	-0.643293	-1.273502
H	-1.217987	3.577383	-0.421467
O	-1.969512	3.391197	0.166686
H	-1.796581	2.431592	0.375164
H	-0.270274	-0.862367	2.530882
O	-0.995436	-0.712396	3.217767
H	-1.394141	0.061791	2.791083
H	3.673755	-0.077403	0.288549
O	3.777788	0.875878	0.127594
H	2.828586	1.147650	0.005906
O	2.922637	-2.026027	0.542728
H	2.093334	-1.548742	0.873628
H	2.634303	-2.269714	-0.353551
H	-0.155911	2.757279	-2.382378
O	0.336728	3.291754	-1.751000
H	0.675326	2.545757	-1.104620
H	-2.568843	-0.235130	0.747211
O	-3.267349	-0.927796	1.024956
H	-2.781629	-1.359581	1.740787
H	-1.621370	-1.558284	-1.569475
O	-2.468263	-2.083762	-1.612897
H	-2.881176	-1.824587	-0.771293

Table S11. Continued

Atom	X / Å	Y / Å	Z / Å
H	0.785122	-3.262794	-1.592066
O	1.366875	-2.600998	-1.979201
H	0.843216	-1.739862	-1.734873

Table S12. Optimized Gas Phase Structure of $PO_4^{3-}(H_2O)_9$ at the B3LYP/6-311++G(d,p) Level

Atom	X / Å	Y / Å	Z / Å
P	0.516960	0.368209	0.539883
O	-0.355058	-0.491800	-0.536720
O	-0.477910	0.960237	1.588269
O	1.271397	1.478070	-0.257663
O	1.483585	-0.650908	1.232135
H	2.654841	-1.426282	0.419193
O	3.282198	-1.927691	-0.202589
H	2.647931	-2.228265	-0.873140
O	-4.039794	-1.501107	-1.093911
H	-3.445142	-1.851458	-0.400596
H	-3.500398	-0.778815	-1.472877
O	-0.434697	3.137938	-1.491009
H	-1.107116	2.469459	-1.693045
H	0.274339	2.577152	-1.042322
O	-2.100394	0.485044	-2.078334
H	-1.383973	0.145922	-1.384119
H	-1.696292	0.231480	-2.913677
O	-1.875112	-2.352104	0.662256
H	-1.312707	-1.666366	0.187241
H	-1.646013	-2.148789	1.586721
O	0.733361	-2.571693	-1.751459
H	0.405273	-1.690678	-1.371499
H	0.332152	-3.181998	-1.123077
O	-0.518921	-1.262314	3.144424
H	0.331288	-1.364397	2.660037
H	-0.731599	-0.365727	2.766084

Table S12. Continued

Atom	X / Å	Y / Å	Z / Å
O	3.852663	0.934887	-1.106163
H	2.944288	1.220927	-0.816713
H	3.833324	-0.006874	-0.865516
O	-1.347050	3.547481	1.413909
H	-1.045762	2.609025	1.574913
H	-1.102954	3.644226	0.478994

Table S13. Gas Phase Electronic Energies and Zero Point Energies of $X(H_2O)_n$ (X = H_3PO_4, $H_2PO_4^-$, HPO_4^{2-}, PO_4^{3-}; n = 7–9) at the B3LYP/6-311++G(d,p) Level of Theory

Cluster	E_o / Hartree	ZPE / kJ·mol^{-1}
$H_3PO_4(H_2O)_7$	-1,179.624 503	594.15
$H_3PO_4(H_2O)_8$	-1,256.092 208	658.41
$H_3PO_4(H_2O)_9$	-1,332.566 807	724.15
$H_2PO_4^-(H_2O)_7$	-1,179.120 671	566.69
$H_2PO_4^-(H_2O)_8$	-1,255.591 463	631.22
$H_2PO_4^-(H_2O)_9$	-1,332.077 629	701.30
$HPO_4^{2-}(H_2O)_7$	-1,178.484 923	534.72
$HPO_4^{2-}(H_2O)_8$	-1,254.974 298	602.07
$HPO_4^{2-}(H_2O)_9$	-1,331.455 167	667.21
$PO_4^{3-}(H_2O)_7$	-1,177.702 875	493.94
$PO_4^{3-}(H_2O)_8$	-1,254.202 621	559.08
$PO_4^{3-}(H_2O)_9$	-1,330.694 252	630.18

Composition of Aqueous Phosphate Solutions – Derivation of Formal Equations.

The experimental pK_a values of phosphoric(V) acid are 2.16, 7.21 and 12.32. The knowledge of these dissociation constants alone is sufficient to predict the concentration of any given form at a specific pH value. This problem may be also approached from another point of view: what is the distribution of species if a single solute is dissolved in water at a given nominal concentration? Both of these questions may be answered simultaneously using the same set of equations. The fundamental relations necessary for resolution of these problems are derived below, assuming activity coefficients equal to 1 for all the reactants considered (the equations are strictly valid for ionic activities only). The relations necessary for resolution of these problems are as follows.

(a) The three dissociation equilibria of H_3PO_4:

$$K_{a,1} = \frac{[H_2PO_4^-][H^+]}{[H_3PO_4]} \qquad (A1)$$

$$K_{a,2} = \frac{[HPO_4^{2-}][H^+]}{[H_2PO_4^-]} \qquad (A2)$$

$$K_{a,3} = \frac{[PO_4^{3-}][H^+]}{[HPO_4^{2-}]} \qquad (A3)$$

(b) The conservation of the total quantity of phosphate:

$$c = [H_3PO_4] + [H_2PO_4^-] + [HPO_4^{2-}] + [PO_4^{3-}] \qquad (A4)$$

(c) The electroneutrality principle and the water autodissociation equilibrium:

$$[H_2PO_4^-] + 2[HPO_4^{2-}] + 3[PO_4^{3-}] + [OH^-] = [H^+] + [K^+] \qquad (A5)$$

$$K_w = [H^+][OH^-] \qquad (A6)$$

Here, c is the total nominal concentration of the phosphate species, while K_w is the ionic product of water (10^{-14} at 25 °C). Square brackets indicate ion concentrations (note that $[H^+]$ is used to simplify the equations, disregarding the actual structure of the hydrated proton).

By solving eqs. (A1-A3) for $[H_2PO_4^-]$, $[HPO_4^{2-}]$ and $[PO_4^{3-}]$, respectively and substituting successively Eq. (A1) into (A2) and then (A2) into (A3), we may eliminate all unknowns apart from

$[H_3PO_4]$ by introducing the transformed Eqs. (A1-A3) into Eq. (A4). Eventually, the concentration of phosphoric acid at any given pH is obtained from:

$$[H_3PO_4] = \frac{c}{1 + \frac{K_{a,1}}{[H^+]} + \frac{K_{a,1}K_{a,2}}{[H^+]^2} + \frac{K_{a,1}K_{a,2}K_{a,3}}{[H^+]^3}} \qquad \text{(A7)}$$

Using this value, one might obtain all other phosphate concentrations again from Eqs. (A1-A3):

$$[H_2PO_4^-] = [H_3PO_4]\frac{K_{a,1}}{[H^+]} \qquad \text{(A8)}$$

$$[HPO_4^{2-}] = [H_3PO_4]\frac{K_{a,1}K_{a,2}}{[H^+]^2} \qquad \text{(A9)}$$

$$[PO_4^{3-}] = [H_3PO_4]\frac{K_{a,1}K_{a,2}K_{a,3}}{[H^+]^3} \qquad \text{(A10)}$$

To calculate the pH of a solution obtained by dissolving a specific $K_n[H_{3-n}PO_4]^{n-}$ (n = 0-3) phosphate in water at nominal concentration *c*, the electroneutrality principle is applied. Namely, $[OH^-]$ is calculated from Eq. (A6), $[K^+]$ is taken as $n \cdot c$, and Eqs. (A8-A10) are substituted for $[H_2PO_4^-]$, $[HPO_4^{2-}]$ and

$[PO_4^{3-}]$. Finally, $[H_3PO_4]$ is taken from Eq. (A7). After rearrangement, the resulting Eq. (A11) eventually allows calculation of $[H^+]$ and thus pH.

$$c\frac{\frac{K_{a,1}}{[H^+]} + 2\frac{K_{a,1}K_{a,2}}{[H^+]^2} + 3\frac{K_{a,1}K_{a,2}K_{a,3}}{[H^+]^3}}{1 + \frac{K_{a,1}}{[H^+]} + \frac{K_{a,1}K_{a,2}}{[H^+]^2} + \frac{K_{a,1}K_{a,2}K_{a,3}}{[H^+]^3}} - n\,c + \frac{K_w}{[H^+]} - [H^+] = 0 \qquad \text{(A11)}$$

Eq. (A11) is conveniently solved numerically until desired convergence is reached, assuming a sensible starting value of $[H^+]$. The tentative starting pH for $K_n[H_{3-n}PO_4]^{n-}$ phosphate is taken as the arithmetic mean of the nearby pK_as:

$$pH_o = 0.5(pK_{a,n+1} + pK_{a,n}) \qquad \text{(A12)}$$

Here, 0 and 14 might be substituted for "virtual" p$K_{a,0}$ and p$K_{a,4}$, respectively. Afterwards, all species concentrations might be evaluated from Eqs. (A7-A10) at the already known pH.

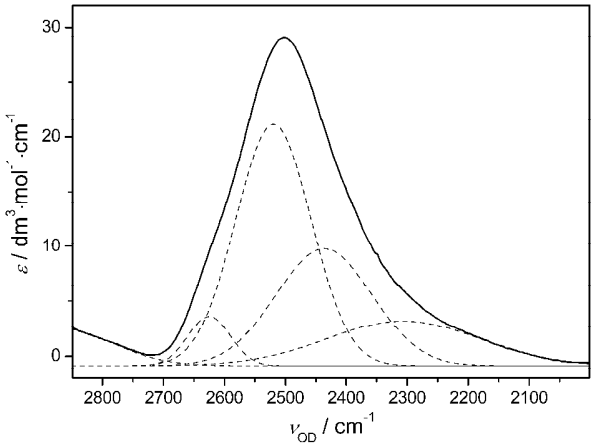

Figure S1. Affected HDO spectrum obtained by subtracting 30% of the original affected HDO spectrum for KH_2PO_4 from the original affected HDO spectrum for H_3PO_4 (solid line) and its decomposition into analytical component bands (dashed lines).

Table S14. Selected Parameters of Analytical Bands from Decomposition of the HDO Spectrum shown in Fig. S1.

solute	ν^{o}_{OD} [a]	ν^{*}_{OD} [b]
H_3PO_4	2625(3)	2625(3)
	2524(12)	2520(10)
	2441(13)	2437(24)
	2310(22)	2307(30)

[a] Original band position at maximum as given in Table 1 (cm^{-1}), uncertainty of fit (as final digits of the value) given in parentheses. [b] Band position at maximum for the component bands shown in Fig. S1 (cm^{-1}), uncertainty of fit as above.

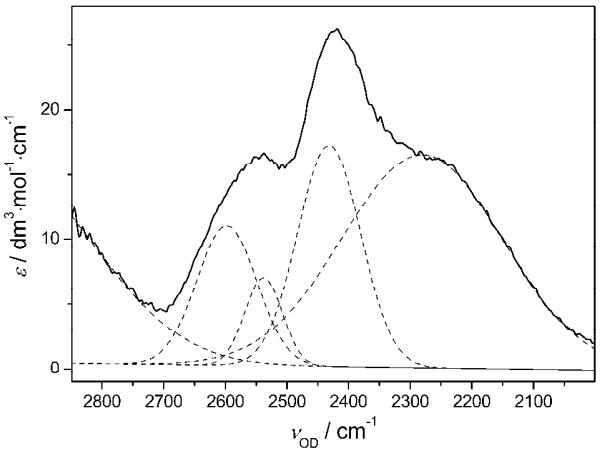

Figure S2. Affected HDO spectrum obtained by subtracting 30% of the original affected HDO spectrum for K_2HPO_4 from the original affected HDO spectrum for K_3PO_4 (solid line) and its decomposition into analytical component bands (dashed lines).

Table S15. Selected Parameters of Analytical Bands from Decomposition of the HDO Spectrum shown in Fig. S2.

solute	ν^{o}_{OD} [a]	ν^{*}_{OD} [b]
K_3PO_4	2602(4)	2598(3)
	2538(12)	2538(12)
	2434(11)	2432(17)
	2301(10)	2280(16)

[a] Original band position at maximum as given in Table 1 (cm^{-1}), uncertainty of fit (as final digits of the value) given in parentheses. [b] Band position at maximum for the component bands shown in Fig. S2 (cm^{-1}), uncertainty of fit as above.